STRESSES IN PIPE ELLS UNDER INTERNAL PRESSURE

RAYMOND J. LE BER
AND
JAMES W. MORRISON

1953

Library
U. S. Naval Postgraduate School
Monterey, California

STRESSES IN PIPE ELLS UNDER INTERNAL PRESSURE

Raymond J. Le Ber
James W. Morrison

STRESSES IN PIPE ELLS UNDER INTERNAL PRESSURE

by

Raymond Jean Le Ber, Commander, United States Navy
James William Morrison, Lieutenant, United States Navy

Submitted in partial fulfillment
of the requirements
for the degree of
MASTER OF SCIENCE

United States Naval Postgraduate School
Monterey, California
1953

L36

This work is accepted as fulfilling
the thesis requirements for the degree of

MASTER OF SCIENCE

from the

United States Naval Postgraduate School

PREFACE

This paper is the result of investigating stresses in five samples of steel pipe bends which were furnished the United States Naval Postgraduate School, Monterey, California, as a result of an offer by Dr. John E. Brock, Research Director, Midwest Piping and Supply Company, St. Louis, Missouri, through Professor Robert E. Newton of the School's Mechanical Engineering Department. It is felt that a good start on this topic has been made in this paper and it is hoped by the authors that the five specimens which remain intact will be made use of in continuing and more extensive research.

The work on this thesis was accomplished in March through May of 1953 at the United States Naval Postgraduate School, Monterey, California, under the direction and guidance of Professor Newton. To him the authors are indebted for all the help and assistance which he has so cheerfully given. To Dr. Brock of St. Louis, not only the authors, but the School also, are indebted for the valuable pipe bends which remain as material for further study.

The authors are also indebted to Captain W. L. Turney, USN, Commander of the San Francisco Naval Shipyard, for the loan of the pump and gage used in the tests.

TABLE OF CONTENTS

		Page
CERTIFICATE OF APPROVAL		i
PREFACE		ii
TABLE OF CONTENTS		iii
LIST OF ILLUSTRATIONS		iv and v
TABLE OF SYMBOLS AND ABBREVIATIONS		vi
PRESENTATION		
I	SUMMARY	1
II	BACKGROUND	3
III	OBJECTIVE	3
IV	SPECIMEN DESCRIPTIONS	5
V	EXPERIMENTAL TECHNIQUES	6
VI	MOUNTING ASSEMBLY	10
VII	CALCULATIONS	12
VIII	COMMENTS	15
IX	CONCLUSIONS	17
X	RELIABILITY OF DATA	17
XI	RESULTS	19
XII	RECOMMENDATIONS FOR FUTURE TESTS	21
BIBLIOGRAPHY		49
APPENDIX		50

LIST OF ILLUSTRATIONS

		Page
Fig. 1	Pipe dimensions	23
Fig. 2	Pressure electric lead transfer block	24
Fig. 3	Gage locations	25
Fig. 4	Measured pipe diameters	26
Fig. 5	Specimen No.1 Symmetrical section, stress to pressure vs. gages on hoop.	27
Fig. 6	Specimen No.2 Transition section, stress to pressure vs. gage on hoop.	28
Fig. 7	Specimen No. 1 Meridian, stress to pressure vs. gage location	29
Fig. 8	Specimen No. 2 Symmetrical section, stress to pressure vs. gage on hoop.	30
Fig. 9	Specimen No. 2 Transition section, stress to pressure vs. gages on hoop.	31
Fig.10	Specimen No.2 Meridian, stress to pressure vs. gage location	32
Fig.11	Specimen No. 3 Symmetrical section, stress to pressure vs. gages on hoop.	33
Fig.12	Specimen No.3 Transition section, stress to pressure vs. gages on hoop.	34
Fig.13	Specimen No.3 Meridian, stress to pressure vs. gage location.	35
Fig.14	Specimen No.4 Symmetrical Section, stress to pressure vs. gages on hoop.	36
Fig.15	Specimen No.4 Transition section, stress to pressure vs. gages on hoop.	37
Fig.16	Specimen No.4 Meridian, stress to pressure vs. gage location.	38

ILLUSTRATIONS - continued

Fig. 17	Specimen No.5 Symmetrical section, stress to pressure vs. gages on hoop.	39
Fig. 18	Specimen No.5 Transition section, stress to pressure vs. gages on hoop.	40
Fig. 19	Specimen No.5 Meridian, stress to pressure vs gage location.	41
Fig. 20	Symmetric sections, mean stress coefficient	42
Fig. 21	Transition sections, mean stress coefficient	43
Fig. 22	Specimen No. 1 Membrane stress to pressure vs. gage location	44
Fig. 23	Specimen No. 2 Membrane stress to pressure vs. gage location	45
Fig. 24	Specimen No.3 Membrane stress to pressure vs. gage location	46
Fig. 25	Specimen No. 4, Membrane stress to pressure vs. gage location	47
Fig. 26	Specimen No. 5, Membrane stress to pressure vs. gage location	48

TABLE OF SYMBOLS AND ABBREVIATIONS

d, d_o, d_i	Diameter of pipe cross section in inches
E	Young's Modulus of Elasticity = 29.6×10^6 p.s.i.
P	Internal pressure in pounds per square inch
R	Mean radius of elbow bend in inches (See Fig. 1)
r, r_i, r_o	Radius of pipe cross section in inches
t	Wall thickness of pipe in inches
$\bar{\epsilon}$	Measured strain - microinches per inch
ϵ	Actual strain - microinches per inch
ν	Poisson's ratio = 0.3
σ	Calculated stress - pounds per square inch
p.s.i.	pounds per square inch

Subscripts:

i	inside surface of pipe
o	outside surface of pipe
t	tangential or hoop direction
l	longitudinal or meridional direction

I. SUMMARY

The objective of this thesis was to obtain a comparison of the stresses present in heavy walled 90° steel pipe elbows under internal hydrostatic pressure. Comparison was achieved using five specimens, grouped as follows:

a) Constant mean radius of bend, varying wall thicknesses - three (3) specimens.

b) Varying mean radius of bend, constant wall thickness - three (3) specimens.

Cemented Baldwin-Lima-Hamilton SR-4 resistance strain gages were used on inner and outer surfaces for measurement of strain. Hydrostatic internal oil pressure was used for loading all specimens. Using Hooke's Law, stresses were computed from the measured strains.

The maximum stress due to internal pressure was for the locations selected found to be on the inside surface at the quarter point of 90° bend in the tangential direction and was greater than either the stress developed at the end or mid-point of the bend. For the thinnest wall (thickness 0.322 inch) specimen the ratio of stress to internal pressure was almost double that calculated by the Lame' formula for straight sections of pipe under internal pressure and half again as much as found from a membrane analysis of a torus.

For the next thickness (0.500 inch) section there were three specimens which showed an increase of about 50 per cent over the Lame' formula and about 30 per cent over the membrane torus analysis.

Within the limits of accuracy of this work, no great deviation from hoop and meridional directions were obtained for the principal stress axes.

Detailed findings are exhibited in graphical form.

II BACKGROUND

From a practical standpoint designers of piping under internal pressure must resort to liberal increases in wall thickness over theoretically required thicknesses. These increases are supplemented for pipe bends and pipe system under unknown external loads. The dangers present with such a system of design were well pointed out by Henry C. E. Meyer [4], His discussion, centered on a warning against overdesign of pipes for high pressure, high temperature steam service, is pertinent to the application studied in this paper, which is concerned with internal hydraulic pressures at room temperatures.

This investigation of heavy-walled 90° pipe ells resulted from an offer by the Director of Research of the Midwest Piping and Supply Co. Inc., St. Louis, Missouri, to the United States Naval Postgraduate School, Monterey, California, to provide the necessary specimens required for a student thesis. The basic need for investigation stemmed from a lack of knowledge of the behavior of thick walled pipe elbows with straight end extensions under internal pressure.

III OBJECTIVE

The main objective of this paper was to develop surface stress and strain data at selected inside and outside locations,

which could provide a basis of comparison with predicted results of established formulae. Selected locations, indicated on Fig. 3, were as follows:

a) Circular cross section of symmetry of the 90° elbow part of each specimen.

b) Circular cross section at point of tangency (end of elbow to straight end).

c) Inside meridional axis (intersection of longitudinal plane of symmetry with inner pipe wall).

d) On outside surface only, a check point in the straight section for comparison with the Lame' solution [8] for the stresses present in a straight section of pipe under internal pressure.

Established formulae used for comparisons are:

1. Lame' solution of straight pipe under internal pressure [8];
2. Membrane analysis for calculating hoop and meridional stresses in a hollow torus under internal pressure [1];
3. Membrane analysis for calculating hoop and meridional stresses in a straight section of pipe under internal pressure [7].

The meridional (longitudinal) stresses given by all three formulas are the same. Formulas are stated in Appendix.

IV SPECIMEN DESCRIPTION

Five steel pipe test specimens numbered 1 to 5 were provided. Nominal dimensions are shown on Fig. 1. Specimens 2 and 4 were made up with seamless welding elbows of nearly constant wall thickness, manufactured by "Tube-Turns", Inc. Specimens 1 and 3 were similarly made with elbows, manufactured by the Taylor Manufacturing Co.

"Tube-Turns" and "Taylor" elbows, in lieu of their own make, were chosen by the Midwest Co. for specimen assembly in the interest of analytic precision. The Midwest elbow contains a longitudinal (meridional) double submerged arc machine weld along the inside radius of the torus and the plate material is preferentially thickened in this region. The elbows supplied are seamless and of more nearly constant wall thickness.

Furnace stress relief anneal was given to specimens 1 to 4, inclusive. Welds were ground smooth inside and outside (not standard commercial practice, but provided in this instance for sake of uniformity of thickness). Specimens 2 and 4 had some rather deep longitudinal inside grooves in the elbows due to manufacturing process. The Midwest Co. dressed these down to a reasonable degree by hand grinding. Specimens 1 and 3 also had some longitudinal grooves to a degree no greater than usual commercial standards.

Pipe in the specimens conformed to the ASTM Specification A-106 Grade B and the elbows to ASTM Specification A-234 (WPB) and to ASA Standard B 16.9. Pipe to elbow circumferential joints were machine arc welded using Oxweld No. 36 rod and Unionmelt No. 80 flux.

Actual dimension and machining accuracy of flanges and bolt circles conformed closely with nominal dimension listed with the exception of Specimen 5. Deviation of pipe cross sections from circularity is indicated in Fig. 4. The bend in No. 5 was made hot with sand filling. Stress relief anneal was not considered necessary.

Two blind flanges were provided by the Midwest Co. One inch shear bolts and standard hexagonal nuts being the only bolts available were used for bolting. One bolt was proof-tested in tension to 32,000 p.s.i. in a universal testing machine prior to use in the tests as a precaution, it being anticipated that that stress would be exerted on each bolt at about 2000 p.s.i. internal pressure.

V EXPERIMENTAL TECHNIQUES

Water was first tried as the pressure medium, but dielectric strength between gages could not be maintained in spite of efforts at insulation. A light cylinder recoil oil which was available

was next tried and proved to be quite satisfactory. Internal pressure was obtained with a Watson-Stillman hand operated pump of 10,000 p.s.i. capacity delivering a maximum of one cubic inch per stroke.

To bring the necessary gage leads through the pressure shell, electrically insulated and pressure tight, a special cemented lucite transfer block was designed. The transfer block was assembled (as shown in Fig. 2), then cemented with Duco cement to the inside face of the blind flange. This transfer block was used with pressures up to 1600 p.s.i. with only a slight amount of leakage.

The flanged joints were made up using fully annealed 1/32 inch thick sheet copper as gaskets for each run. Twelve one inch shear bolts were used per flanged joint. All bolts were set up in a skip sequence with a torque wrench using step increments of torque per sequence until all bolts were estimated to be at 25,000 p.s.i. stress at 2000 p.s.i. internal pressure (300 ft. lbs. torque on each bolt [9]). Generally, the leakage through the gasketed joints prevented using pressures in excess of 1600 p.s.i.

A dead weight gage tester was used to establish precise pressure control. The gage tester was used in conjunction with

the pump to produce a known pressure. Deadweights available produced "gage" pressures of 418, 818, 1218, and 1618 p.s.i. These pressures were used to calibrate a tangential element of one of the SR-4 strain gages. This gage was connected to a separate strain indicator and the combination strain gage and indicator was used as a precise pressure control device.

A Bourdon type pressure gage of 10,000 p.s.i. capacity was used for initial pressure build-ups to region of deadweight calibration pressures.

Surface preparation, inside and outside, was accomplished using power wire brushes, emery cloth, and carbon tetrachloride followed by acetone as cleaning agents. The strain gages were cemented to surfaces by hand pressure only using a Duco cement. The gages on the inside surfaces were not coated, with the exception of a few gages on specimen No. 1 which were covered with petrosene wax, use of which was discarded as unnecessary when oil was adopted as the pressure medium. Water proofing of the gages on the outer surfaces was deemed unnecessary due to the relatively stable atmospheric conditions prevailing inside the test laboratory.

Strains were obtained using SR-4 strain gages. Two element gages (AX-5) were used in locations where the principal stress

directions were known from the symmetry of the structure. Three element gages (AR-1) were used in remaining locations. Fig. 3 shows the gage locations and numbering sequence. Gages were numbered to indicate location on each specimen with inside gages numbered 1 to 12, and outside gages numbered 21 to 33. Gages 1 to 5 were located on the inside cross section of symmetry. Gages 21 to 25 were in corresponding outside sections. Gages 6 to 10 were located on the inside cross section at change from curved section to straight section; with gages 26 to 30 in corresponding outside locations. These gages were spaced at 45° angles from a 0° meridian to the 180° meridian (shown on Fig. 3). Gages 11 and 31 were inside and outside between gages 1, 21 and 6, 26. Gages 12 and 32 were at a location equidistant on the 20° meridian from gages 6 and 26 as 11 and 31. Gage No. 33 was on the 90° meridian, 6 inches distant from the transition cross-section on the straight pipe.

The AX-5 compensator gage was mounted on a small steel flat bar 3 inch x $1\frac{1}{2}$ inch x $\frac{1}{4}$ inch thick. One element of this gage was used in the bridge circuit.

Gage positioning was accomplished by level alignment of specimens to determine locations. Meridian centerlines were established in this way and the flange faces were used to locate hoop planes. Inside gages were located using masking tape

suitably located and marked to provide guide lines. The inside gages' leads were soldered prior to cementing. Due to working space limitations, it was necessary to use flexible gage leads to permit manipulation of the gages in order to obtain precise placement of the gage elements. For this reason inside gage leads were of 28 mil enameled copper wire. Mirrors were used for verification of the interior locations. The gages on the outside surface were located and cemented without difficulty. The outside gage leads, of 40 mil tinned and woven cloth covered copper wire, were soldered to the gages after cement was set and thoroughly dried. Suitable marker tags identified the gage leads. These consisted of gage number and the subscript letters "l" and "t" for the two element gages to indicate the longitudinal and transverse directions. The subscripts "A", "B" and "C" were used to denote the individual elements of the three gage rosettes. (see Fig. 3).

VI MOUNTING ASSEMBLY

Upon completion of the strain gage installation the elbows were mounted for testing. It was necessary to mount the specimens in a manner to preclude the introduction of stresses other than those produced by the internal pressure. This was accomplished by resting one leg of the specimen horizontally and the other standing

vertical and free to move except for loose side guides to prevent tipping. The horizontal leg was secured with a strap.

The flange on the horizontal leg was first bolted up. The gage leads were then connected to the transfer block on the other flange for the vertical leg. The vessel was next filled with oil until almost full, the second flange bolted tight, and filling resumed, venting through the pipe lead to the deadweight gage tester.

Two Baldwin Type K strain indicators were used to obtain data, one used as a pressure indicator and the other to obtain strains. Two Baldwin SR-4 switching and balancing units were used to facilitate switching and zero adjusting.

The use of a compensator gage on the inside with the inside active gages precluded the use of the zero adjusting feature of the balancing units. For runs involving inside gages, the switching and balancing units were used only as channel selectors. The dummy inside gage was directly connected to the strain indicator for all such runs.

Before any test data were recorded, specimens were "exercised" from atmospheric to a maximum pressure of about 1600 p.s.i. and down to atmospheric for four or five cycles.

The pressure control gage element was calibrated using the deadweight gage tester. Cycling was employed to obtain con-

sistent readings in a linear range of the control element. Once calibration was established, the control element readings were used for pressure determination.

Outside gage data were obtained by ascending step increments of pressure from atmospheric to final pressure and back to atmospheric in descending step increments. Repeated runs were made until it was determined good data were recorded.

Inside gage data were not as reliable as for outside gages. There was a tendency for inside readings to zero-drift and hence the following procedure was followed. After exercising the specimen with pressure from zero to 1600 p.s.i., pressure was applied for each run in the rollowing sequence:

pressure	
0	record gage strains
test	record gage strains
0	record gage strains

The new zero was used for each run. When a consistent set of readings were obtained, the next higher test pressure was used in the run. About four runs were required for each test pressure per specimen to obtain data considered suitably consistent.

VII CALCULATIONS

Standard procedures for obtaining stresses from observed strains, using wire resistance strain gages are presented in

Lee [3] and in many papers in the field of experimental stress analysis. For obtaining stresses present at the outer surfaces the authors used the method as presented by Lee [3]. Plots were made of strain readings Vs pressure from zero to ascending pressure increments, down again to zero in descending increments. When consistent readings were obtained the average apparent strains to pressure ratios were obtained for longitudinal and tangential elements of the AX-5 gages and for the A, B, and C directions of elements for the AR-1 gages. The A and C directions corresponded to tangential and longitudinal directions. Then knowing

$$\epsilon_t = \bar{\epsilon}_t - \frac{\bar{\epsilon}_\ell}{30} \quad ; \quad \epsilon_\ell = \bar{\epsilon}_\ell - \frac{\bar{\epsilon}_t}{30}$$

we calculate (Lee [3]).

$$\sigma_t = \frac{E}{1-\nu^2}(\epsilon_t + \nu\epsilon_\ell)$$

$$\sigma_\ell = \frac{E}{1-\nu^2}(\epsilon_\ell + \nu\epsilon_t)$$

For the rosette gages

$$\epsilon_A = \bar{\epsilon}_A - \frac{\bar{\epsilon}_c}{45} \quad ; \quad \epsilon_c = \bar{\epsilon}_c - \frac{\bar{\epsilon}_A}{45}$$

$$\epsilon_B = 1.02\,\bar{\epsilon}_B - \frac{1}{45}(\bar{\epsilon}_A + \bar{\epsilon}_c)$$

$$\sigma_t = \frac{E}{2}\left[\frac{\epsilon_A + \epsilon_c}{1-\nu} + \frac{1}{1+\nu}\sqrt{2(\epsilon_A - \epsilon_B)^2 + 2(\epsilon_B - \epsilon_c)^2}\right]$$

$$\sigma_\ell = \frac{E}{2}\left[\frac{\epsilon_A + \epsilon_c}{1-\nu} - \frac{1}{1+\nu}\sqrt{2(\epsilon_A - \epsilon_B)^2 + 2(\epsilon_B - \epsilon_c)^2}\right]$$

For interior gages due to the influence of pressure on the compensating gate, a departure from the above was necessary. The inside active gage leads and the compensator lead were in effect directly connected to the Baldwin SR-4, model K, strain indicator and differential strain readings were obtained. Since these strains included the effect of direct hydrostatic compression on the compensator gage, correction for this effect was required. Kooistra and Blaser [2] and O'Brien and Wetterstrom [5] indicate the procedures required in detail.

Briefly, after finding the strains uncorrected for pressure effects, we obtain the corrected stresses:

$$\frac{\sigma_t}{P} = \frac{E}{P(1-\nu^2)}\left[\epsilon_t + \nu\epsilon_\ell\right] - 1$$

$$\frac{\sigma_\ell}{P} = \frac{E}{P(1-\nu^2)}\left[\epsilon_\ell + \nu\epsilon_t\right] - 1$$

Sample plots of inside and outside strain readings are included in the appendix.

The stresses computed from the above relations are presented in graphical form in Figs. 5-19. A membrane theory for the stresses in a hollow torus under internal pressure is presented by Foepl [1]. The membrane stresses on the wall at a point is given by one half the sum of the stresses inside and outside at that point [6]. These observed membrane stresses are compared with the stresses present in a torus under internal pressure in Figs. 22- 26. By multiplying the observed membrane stresses by the nominal wall thickness and dividing by the inside radius, we obtain a dimensionless value showing the relative stresses at each point; the value of unity corresponding to the simple tangential membrane stress; and the value 0.5 corresponding to the longitudinal stress in a thin-walled cylindrical pressure vessel. This relation is plotted for comparison of the stresses present in individual specimens (see Figures 20 and 21).

VIII COMMENTS

The Watson Stillman hand pump presented no major difficulty. The leather plunger wore out under repeated use. A substitute was devised from a section of leather transmission belt. For future tests a replacement supply of hydraulic leathers is recommended.

Flange joints leaked at about 1600 p.s.i. Improvement can be effected by using higher strength bolts and a thicker copper gasket (1/16 inch recommended).

Data obtained from exterior gages were generally considered reliable.

Data obtained from interior gages were generally acceptable but did not conform to nice regularity obtained from exterior gages. There was a continued hysteresis effect noted on interior readings. Possible sources for this effect are:

1. Progressive work hardening of interior copper leads under effect of pressure.

2. Variation in thickness of cement. Gages were cemented in interior of specimens under difficult conditions. Interior surfaces were cleaned as effectively as possible but surface smoothness was not as good as the exterior, although generally smooth enough for proper cementing of gages. Kooisha and Blaser [2] reported similar difficulty.

Efforts to eliminate the above effects included cycling before reading -- the testing of outside gages first contributed to this cycling. All interior readings were from a zero to test pressure in each case.

IX CONCLUSIONS

The principal planes of surface stresses computed from strain indications considered reliable remain normal to the hoop tangent and the meridional axes for any meridian around the hoop at the junction of elbow to parallel end section.

For true circular cross sections it is likely that the maximum stress for the specimens tested occurs along the inside surface of the meridional section in the plane of axial symmetry. (See location 11, Fig. 3). From this paper the indications are that the maximum stress is tangential and lies close to the quarter length cross section, i.e., the section midway between the symmetrical and tangential sections, of the elbow along this meridien.

At the symmetrical and transition cross sections, maximum stresses exist as above on the zero meridian but are lower in value.

When cross sections are not true circles higher bending stresses are induced under internal pressure. These stresses can well go high enough due to ovality to be three times what might be expected.

X RELIABILITY OF DATA

The maximum error in computation of stresses for outside

gages (where data has been noted as reliable) is estimated to be of the order of 4 per cent.

The maximum error in computation of stresses for inside gages (where data has been noted as reliable) is estimated to be of the order of 11 per cent.

An integration of mean longitudinal stresses over a cross section yields an equilibrium check which when compared to internal pressure over the cross section yields the following comparison:

Table I. % of error of equilibrium checks based on summation of longitudinal stresses equated to internal pressure over nominal cross sectional area.

Specimen	Symmetric Section	Transition Section
1	2.5	1.3
2	14.1	4.1
3	11.85	-
4	13.5	-
5	-	2.9

XI RESULTS

Table II compares the maximum tangential stress-to-pressure ratios ($\sigma t/P$) as computed from the Lame' formula, the membrane torus equation, and as obtained in these experiments.

Specimen No.	Wall thickness (inches)	Band Radius (inches)	Lame'	Torus	Experimental	Meridian	Cross Section
1	0.322	12	12.75	16.28	24.9	0°	22½°
2	0.500	12	8.08	10.1	12.9*	0°	22½°
					13.03	90°	0°
3	0.906	12	4.31	5.25	6.32	0°	22½°
4	0.500	8	8.08	12.4	13.6	0°	22½°
5	0.500	28	8.08	8.87	15.9**	0°	22½°

* two locations given due to closeness of data.
** influenced by ovality of the cross section.

Table II Comparison of Maximum Experimental Stresses with the Lame' and torus solutions.

Table III compares the tangential stress to pressure ratio as computed from the Lame' solution for the outside surface (thick cylinder under internal pressure only) and as obtained in these experiments at location No. 13 (Fig. 3). These

results indicate that this gage was in a region of disturbance (with the exception of specimen No. 2).

Specimen No.	Stress/ Pressure	
	Lame'	Experimental
1	11.6	12.60
2	7.07	7.01
3	3.32	3.50
5	7.07	5.06*

Note: Specimen No.4 - unreliable data.

* Stress affected by ovality of cross section.

Table III Comparison of stresses found at Location No. 13 to the stress found in an undisturbed region.

Calculation of principal stress directions at locations 7, 8, 9 inside and outside on the transition cross section, showed no marked deviation from the meridional and cross-sectional directions. Within the limits of experimental error present in these tests, principal stress directions are considered as being close to meridional and tangent to the hoop section.

Figures 5-19 represent the evaluation of stress-to-pressure-ratios for each specimen.

Figure 12 indicates results for specimen No. 3 which were obtained but the results are considered unreliable except at end points (i.e. 0° and 90° meridian).

Dashed lines indicate an estimate where experimental data were considered unreliable.

Figures 20 and 21 represent graphic interpretations of results analyzing specimens 1, 2 and 3, comparing specimens of same nominal bend radius, but of progressively increasing wall thickness. Figures 16 and 17 represent comparisons at the symmetric and transverse cross sections for a "mean stress coefficient", which is defined as $\frac{\sigma_\theta + \sigma_t}{2p} \times \frac{2t}{d_i}$. For the tangential stress the value of this coefficient computed by simple membrane theory is unity. For the longitudinal stress this coefficient equals 0.5.

Figures 22-26 compare the average membrane stress-to-pressure ratios for cross sections and membrane stress-to-pressure-ratios computed by the member torus theory to location points on the meridians of each specimen.

XII RECOMMENDATIONS FOR FUTURE TESTS

Considerable leakage was encountered at the higher internal pressures. The use of better bolts and thicker gaskets would eliminate flange leakage. The electrical lead transfer block can be redesigned to eliminate leakage, a proven practical design being given by Kooistra and Blaser [2].

Projects using a single specimen only could result in greater detail coverage. Data produced in this investigation covered but two cross sections and one meridian. Indications are that the 0° meridian is the most highly stressed line, but only 4 points were covered in this series. Inasmuch as outside gages were more reliable, a relationship using a greater ratio of outside to inside gages could produce acceptable results capable of accurate interpretation.

The 28 inch bend radius specimen (No.5) would be useful for comparison with Specimens 2 and 4 if some means could be found to roll out the ovality. The original intent of comparison had to be abandoned due to this ovality.

The operation of the strain gages on the inside surfaces was in general poor. There is a definite need for further research in this field. This research could be aimed at developing technique and determining the actual effect of hydrostatic pressure on the action of the strain gages.

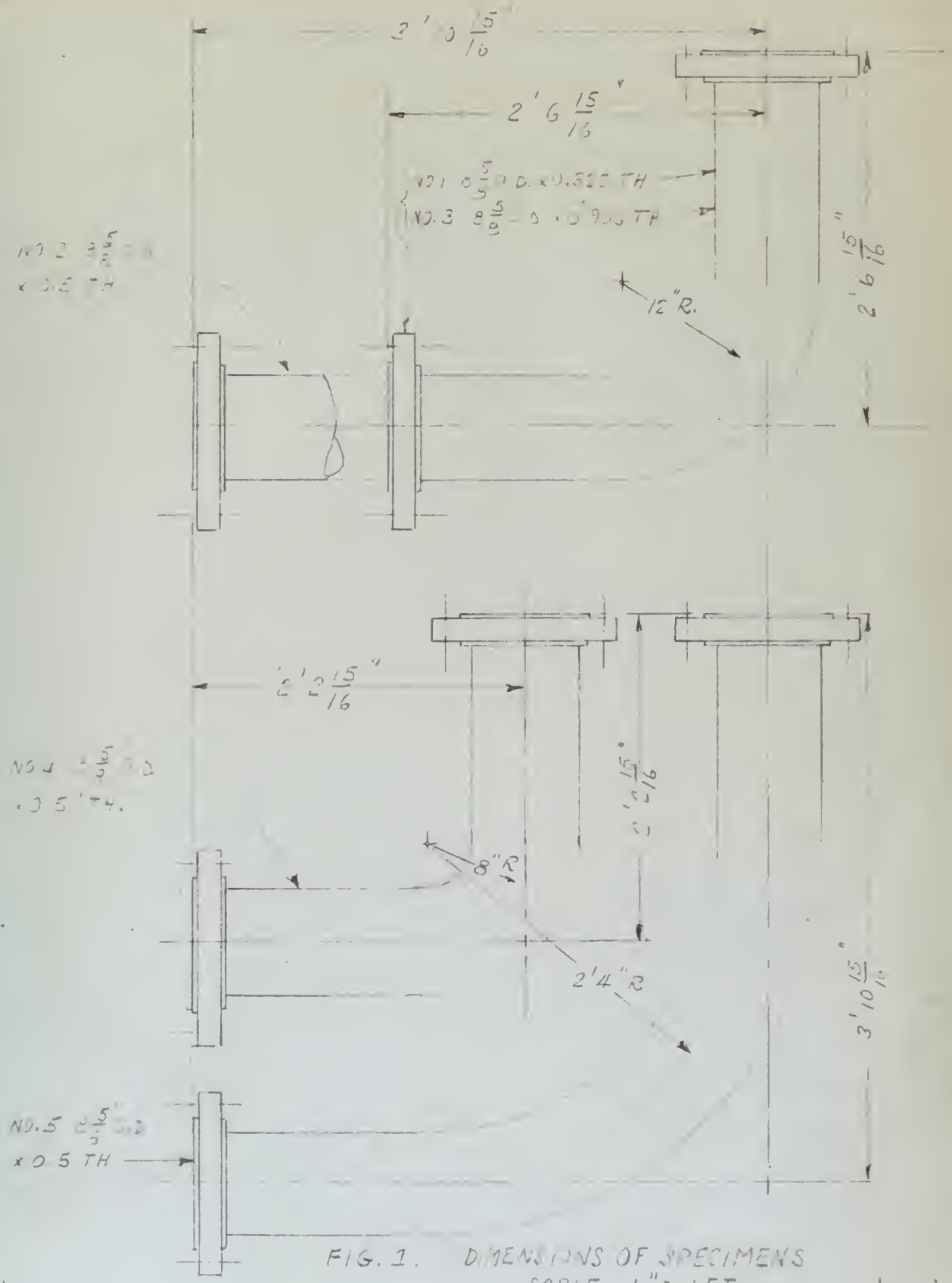

FIG. 1. DIMENSIONS OF SPECIMENS
SCALE 1" = 1 FT.

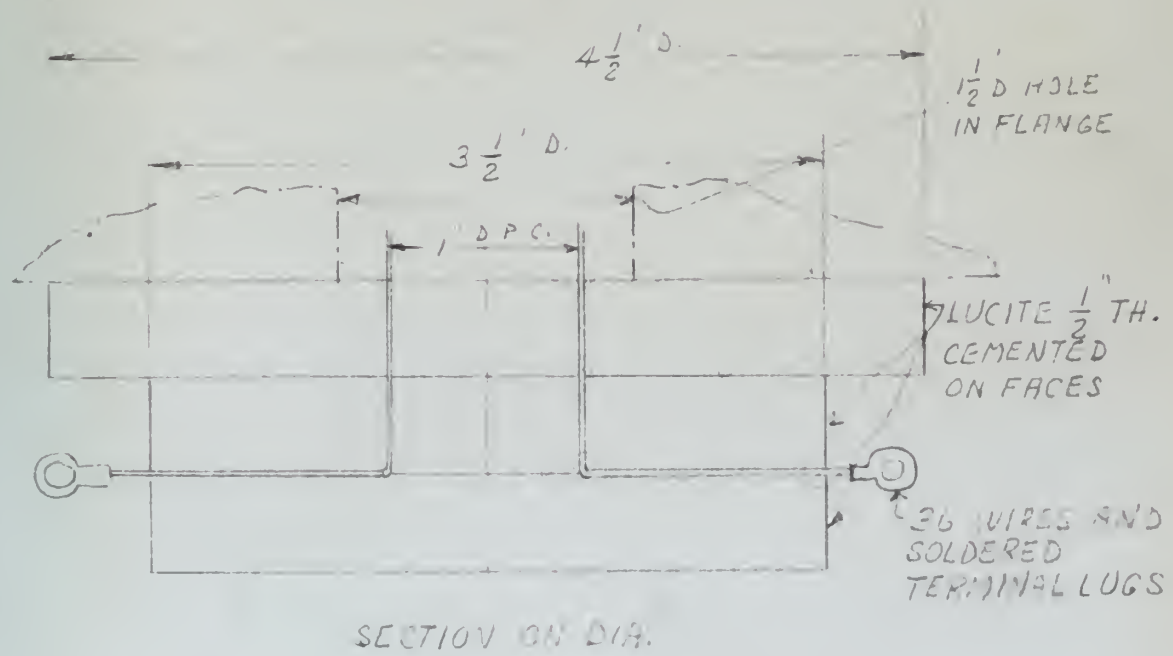

FIG. 2 LUCITE ELECTRIC LEAD PRESSURE TRANSFER BLOCK FOR INSIDE GAGE LEADS TO OUTSIDE TERMINALS

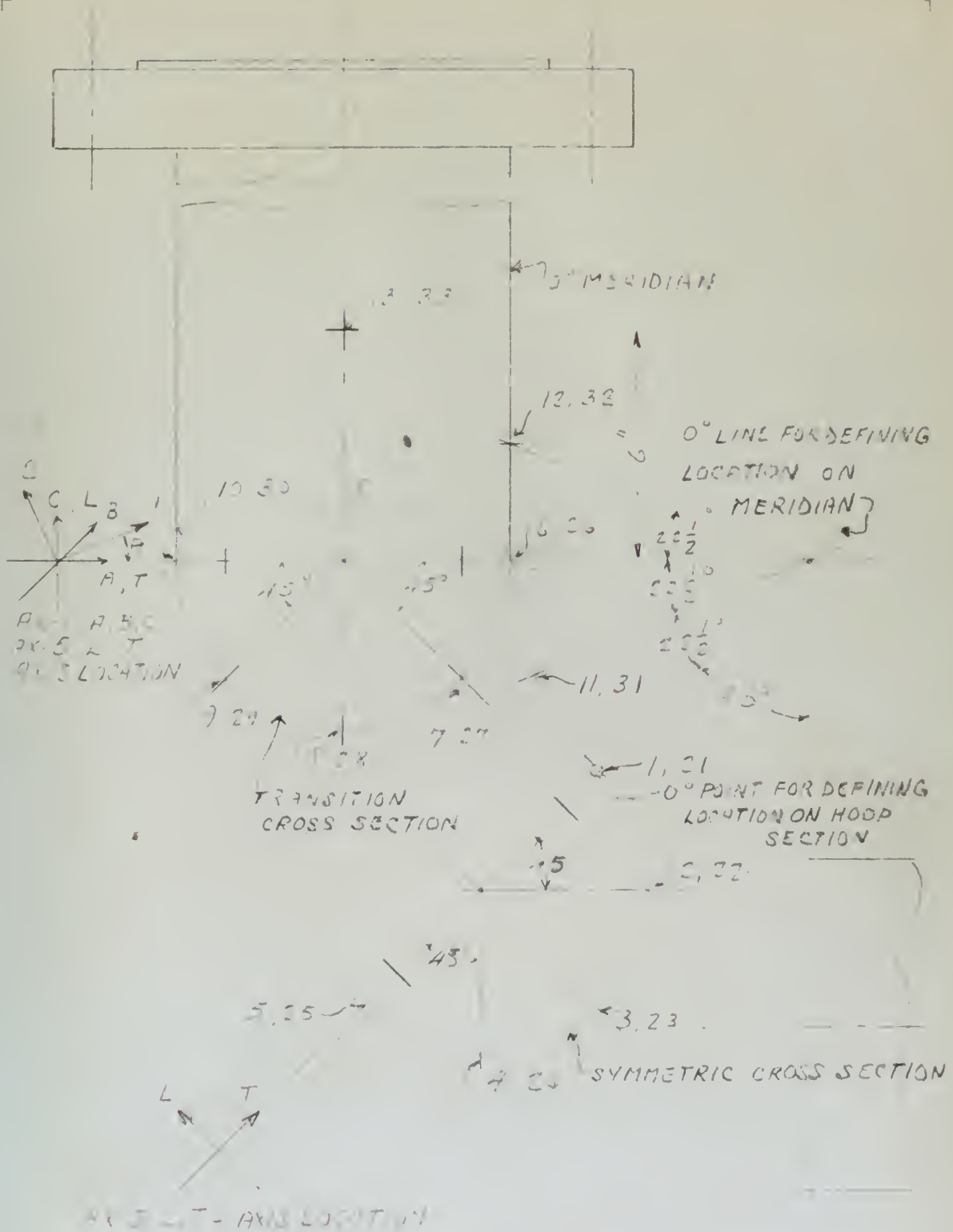
0° MERIDIAN
12, 32
0° LINE FOR DEFINING LOCATION ON MERIDIAN
C, L
B
A, T
10 30
11, 31
7 27
1, 21
TRANSITION CROSS SECTION
0° POINT FOR DEFINING LOCATION ON HOOP SECTION
5, 22
3, 23
SYMMETRIC CROSS SECTION
L
T

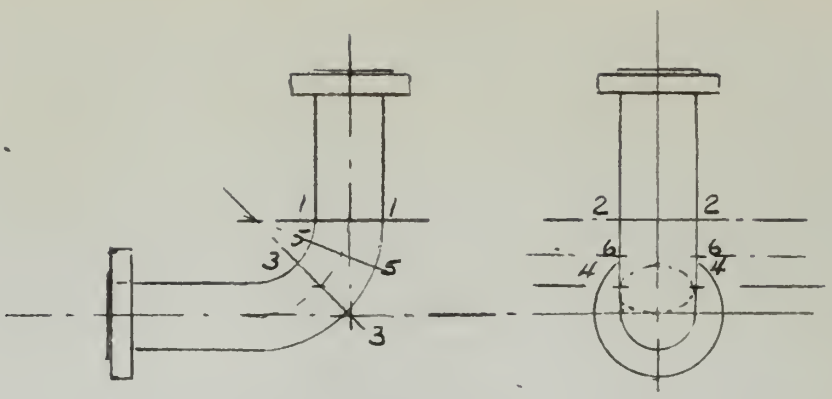

DIAGRAM OF LOCATION POINTS

SPECIMEN \ DIA. AT	1-1	2-2	3-3	4-4	5-5	6-6
1	$8\frac{21}{32}$	$8\frac{19}{32}$	$8\frac{21}{32}$	$8\frac{19}{32}$	$8\frac{3}{4}$	$8\frac{9}{16}$
2	$8\frac{5}{8}$	$8\frac{19}{32}$	$8\frac{21}{32}$	$8\frac{5}{8}$	$8\frac{5}{8}$	$8\frac{9}{16}$
3	$8\frac{21}{32}$	$8\frac{21}{32}$	$8\frac{13}{16}$	$8\frac{3}{4}$	$8\frac{3}{4}$	$8\frac{3}{4}$
4	$8\frac{5}{8}$	$8\frac{19}{32}$	$8\frac{5}{8}$	$8\frac{9}{16}$	$8\frac{9}{16}$	$8\frac{5}{8}$
5	$8\frac{35}{64}$	$8\frac{5}{8}$	$8\frac{3}{8}$	$8\frac{27}{32}$	$8\frac{13}{32}$	$8\frac{29}{32}$

FIG. 4. VARIATION OF OUTSIDE DIAMETERS

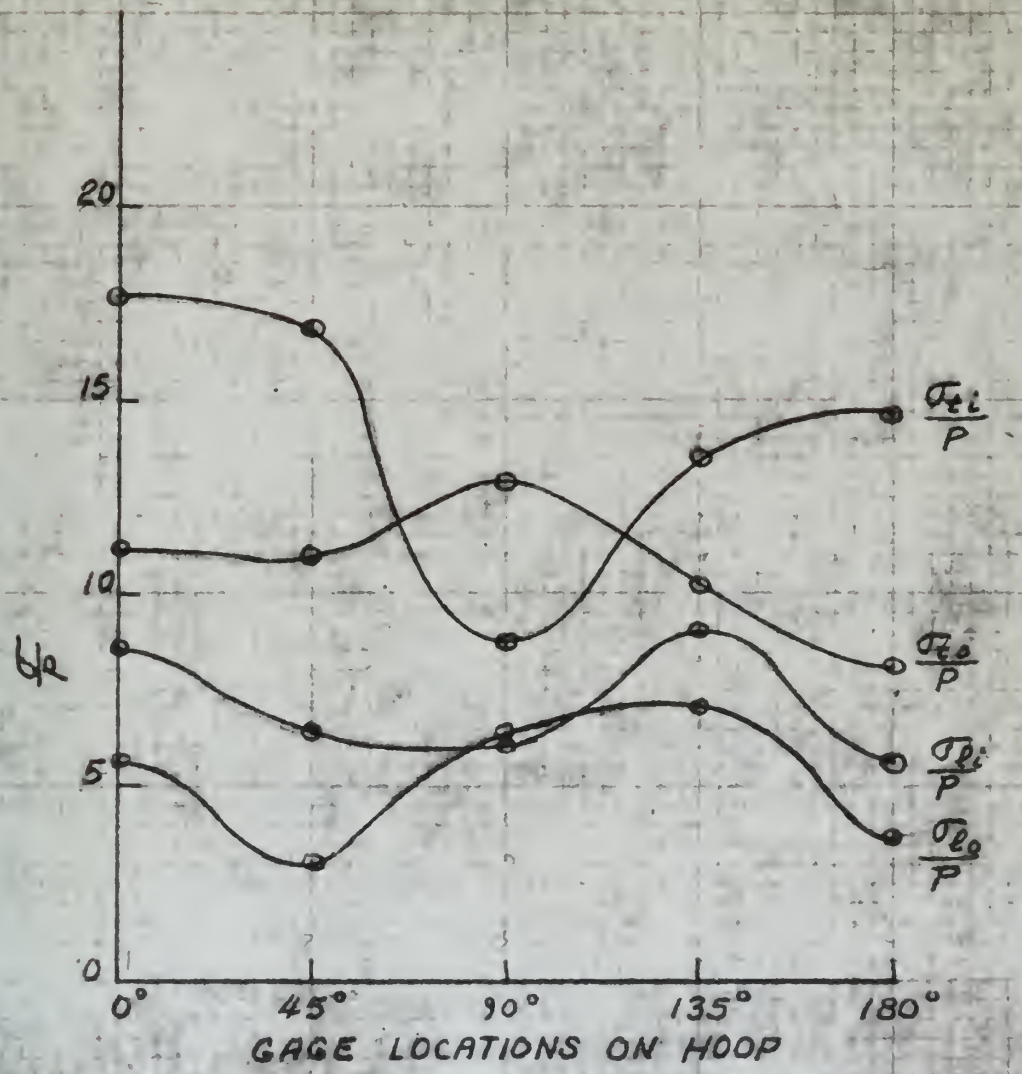

FIG. 5. SPECIMEN NO. 1 SYMMETRICAL CROSS SECTION
STRESS TO PRESSURE VS. GAGE LOCATION

FIG. 5

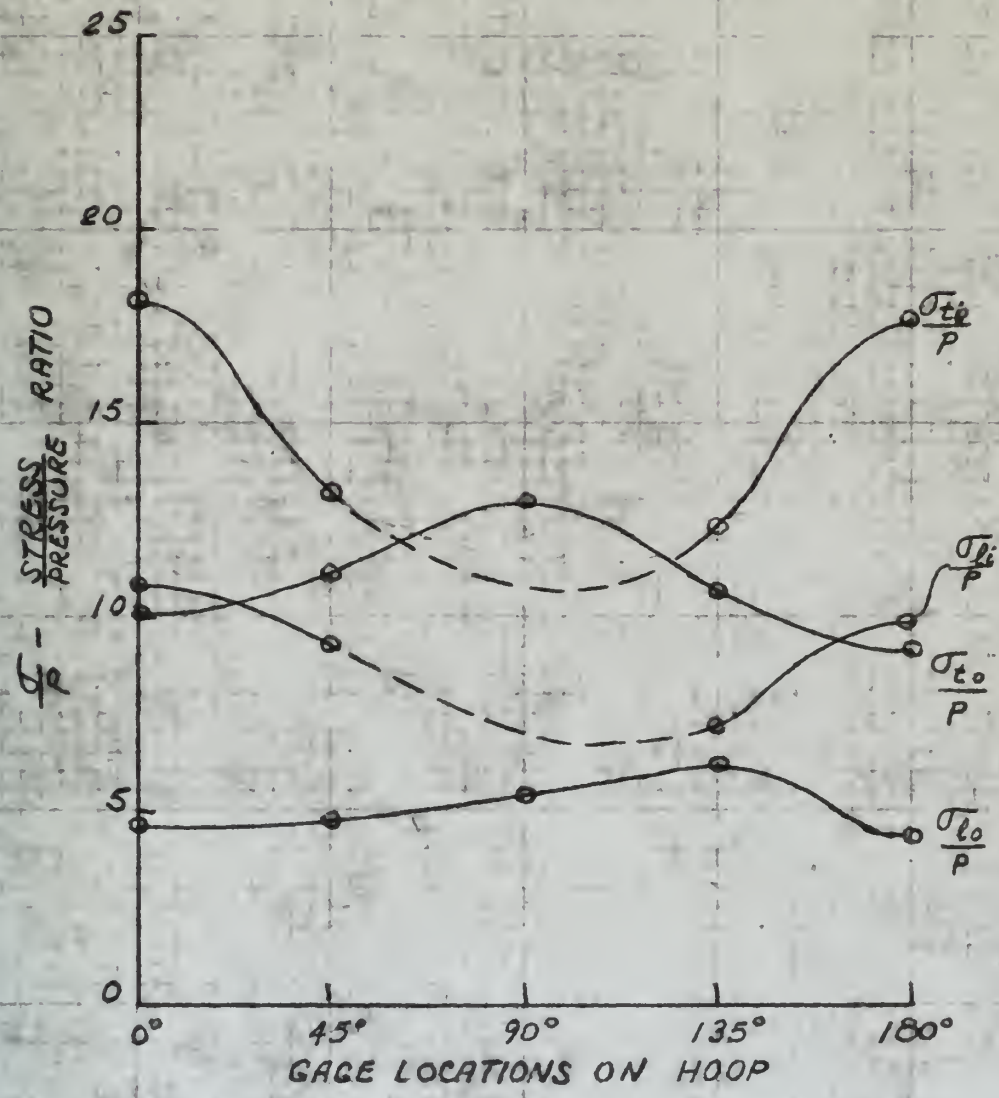

FIG. 6. SPECIMEN NO. 4 TRANSITION CROSS SECTION STRESS TO PRESSURE VS. GAGE LOCATION

FIG. 6

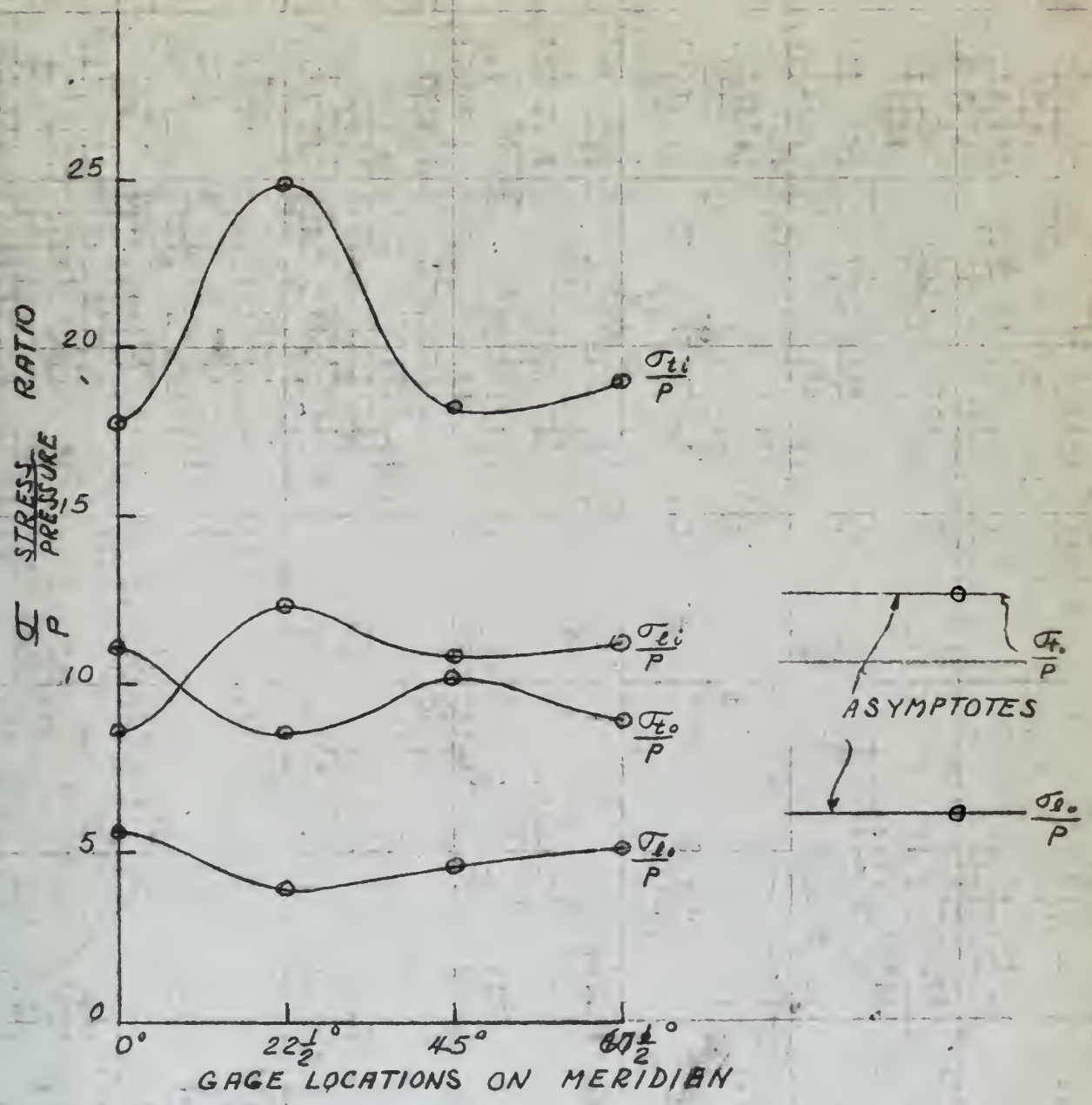

FIG. 7. SPECIMEN NO. 1 0° MERIDIAN
STRESS TO PRESSURE VS GAGE LOCATION

Fig. 7.

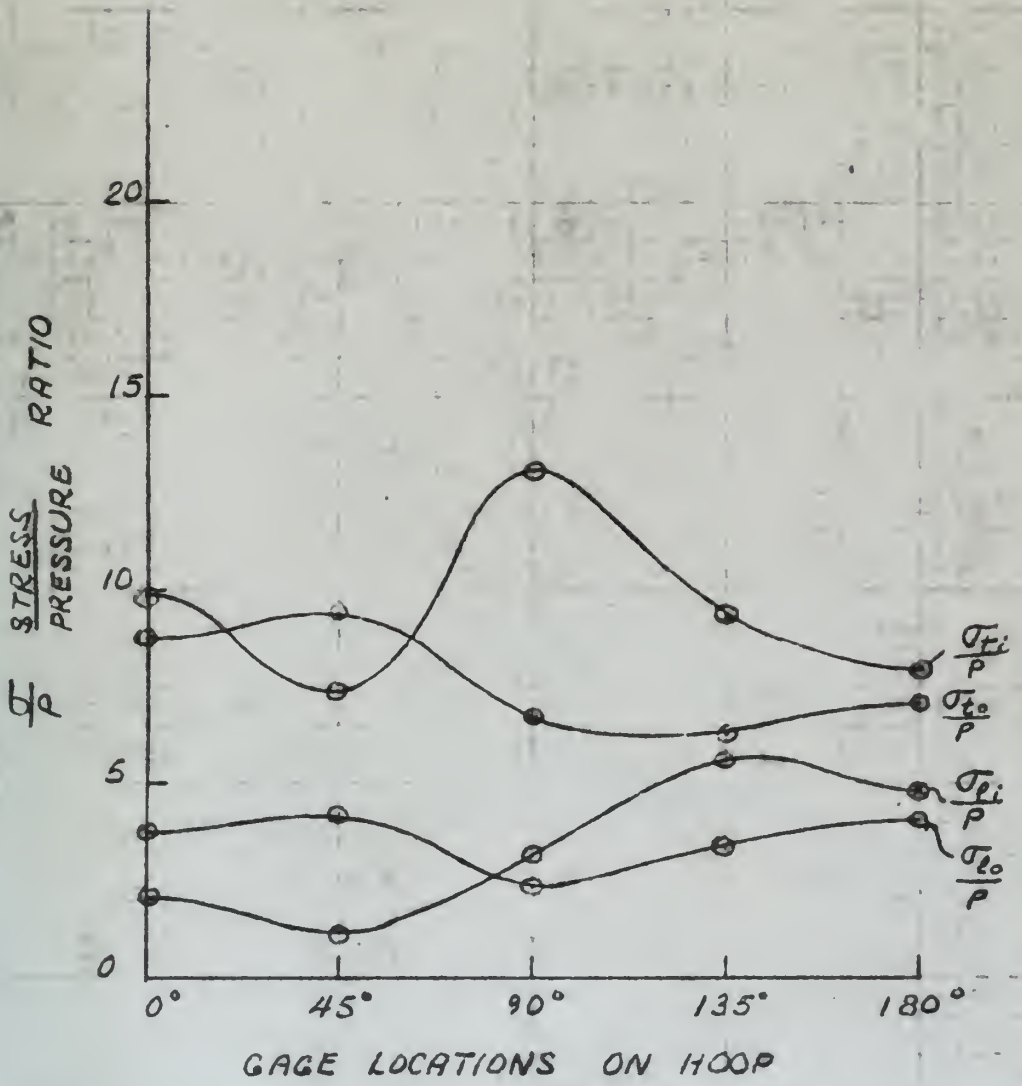

FIG. 8. SPECIMEN NO. 2 SYMMETRICAL CROSS SECTION
STRESS TO PRESSURE VS. GAGE LOCATION

FIG. 8.

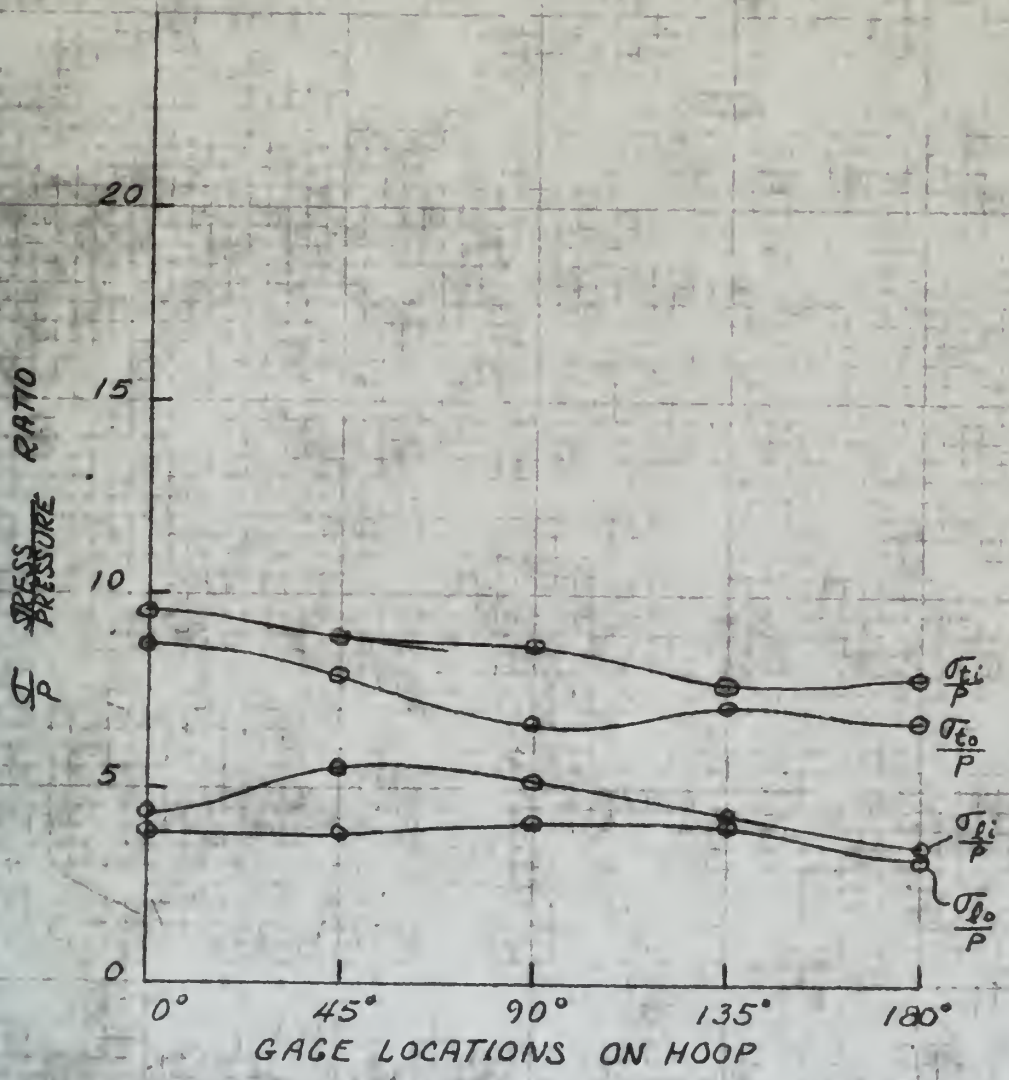

FIG. 9. SPECIMEN NO. 2 TRANSITION CROSS SECTION STRESS TO PRESSURE VS. GAGE LOCATION

FIG. 9

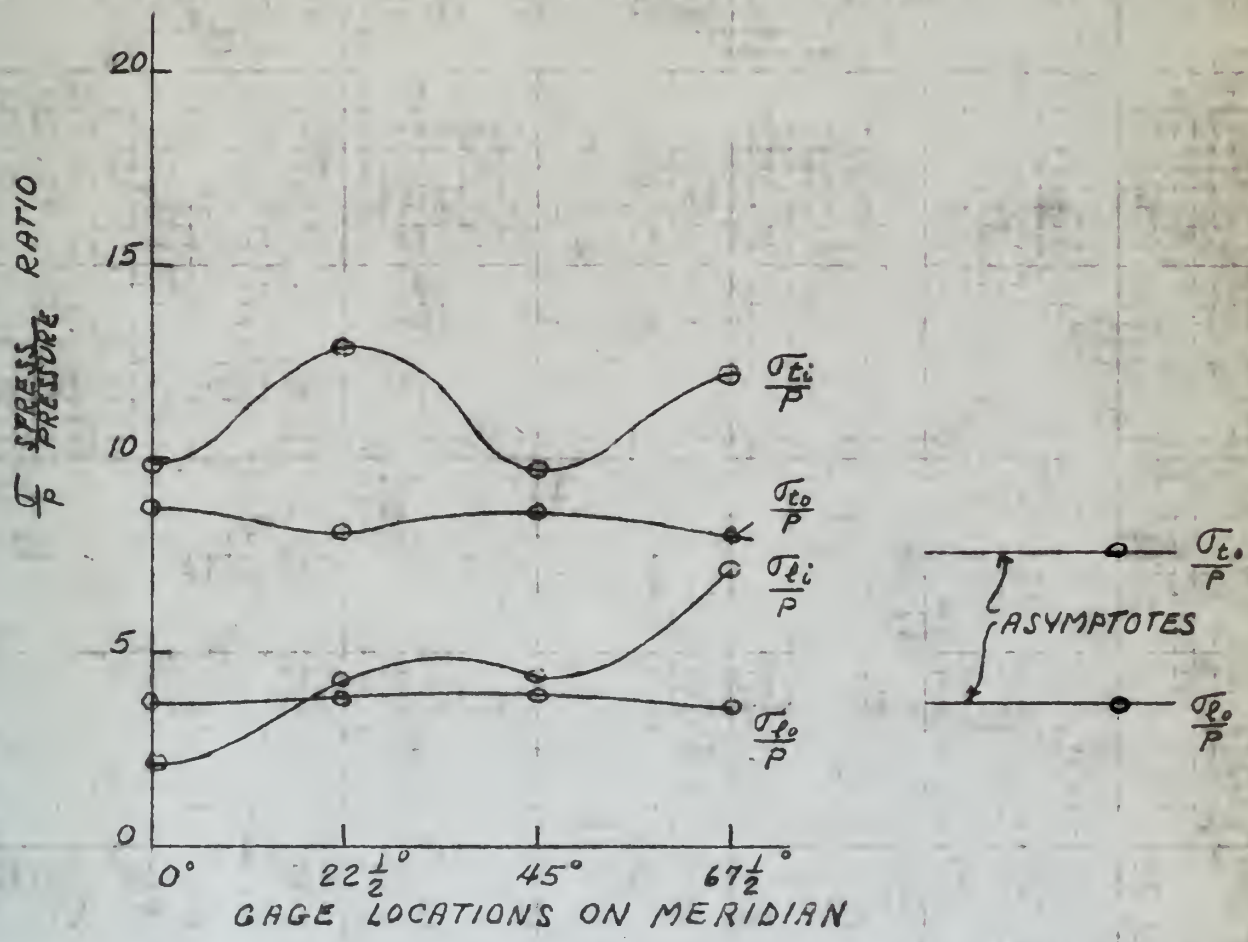

FIG.10. SPECIMEN NO. 2 0° MERIDIAN
STRESS TO PRESSURE VS. GAGE LOCATION

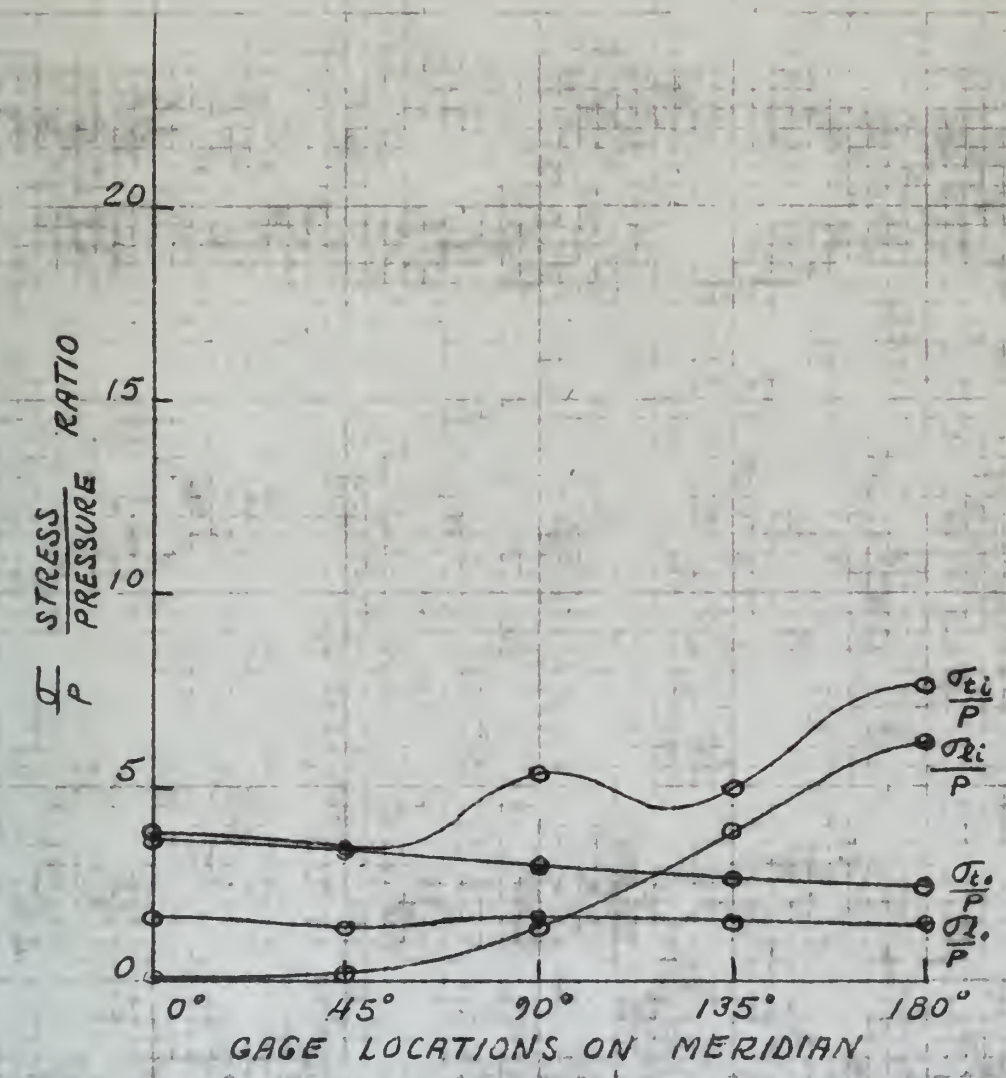

FIG. 11. SPECIMEN NO. 3 SYMMETRICAL CROSS SECTION
STRESS TO PRESSURE VS. GAGE LOCATION

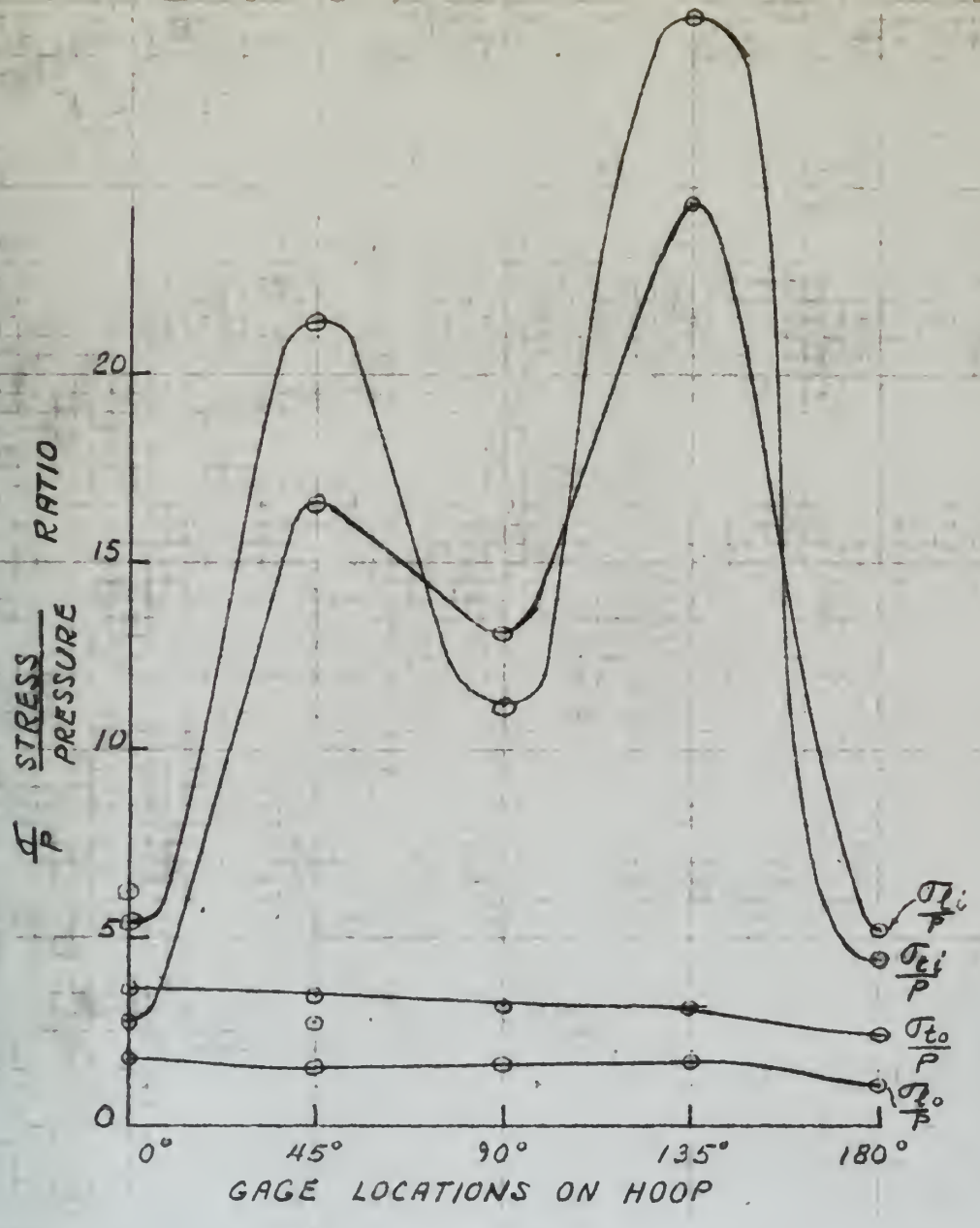

FIG. 12. SPECIMEN NO. 3 TRANSITION CROSS SECTION STRESS TO PRESSURE VS. GAGE LOCATION

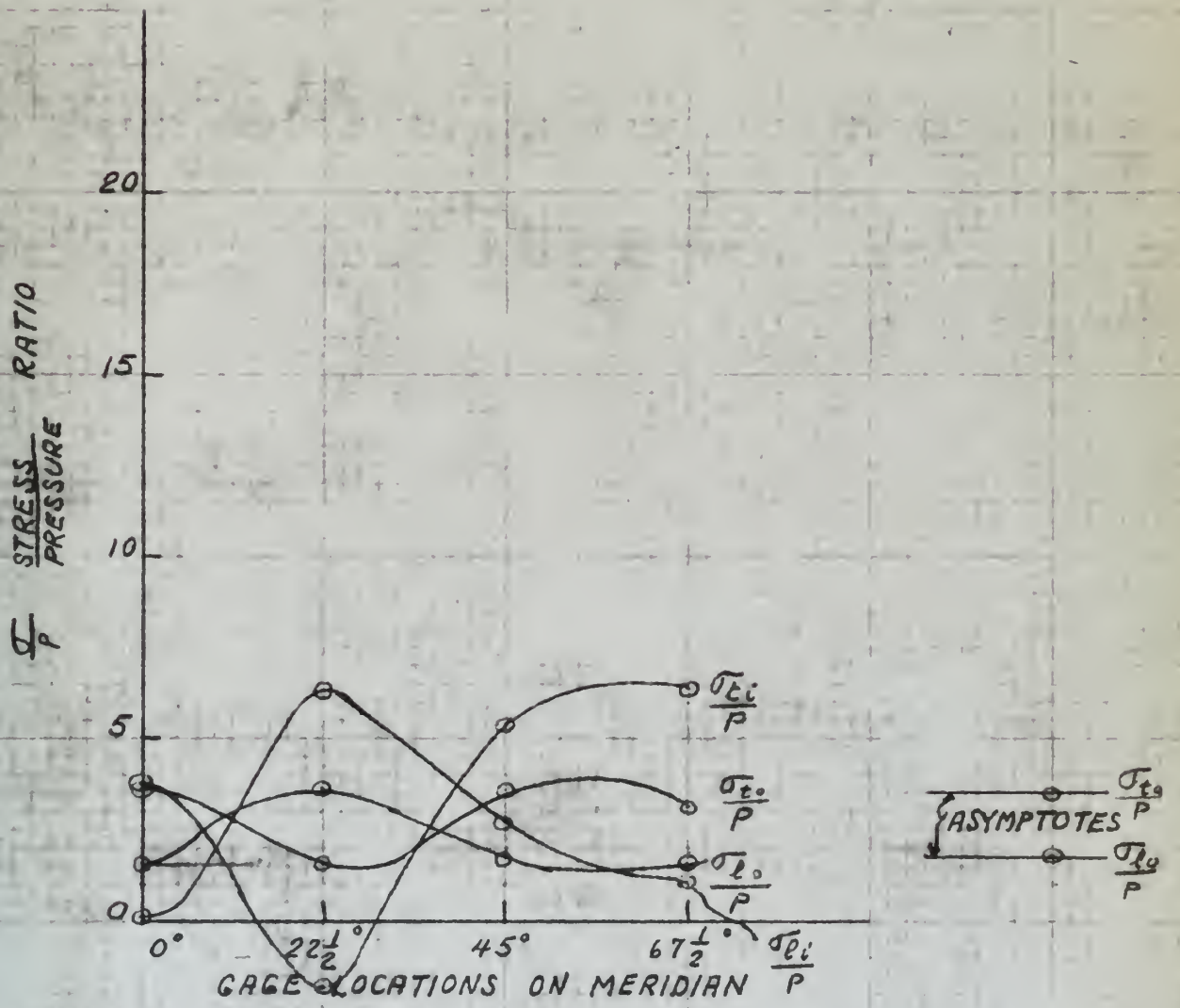

FIG. 13. SPECIMEN NO. 3 0° MERIDIAN
STRESS TO PRESSURE VS. GAGE LOCATION

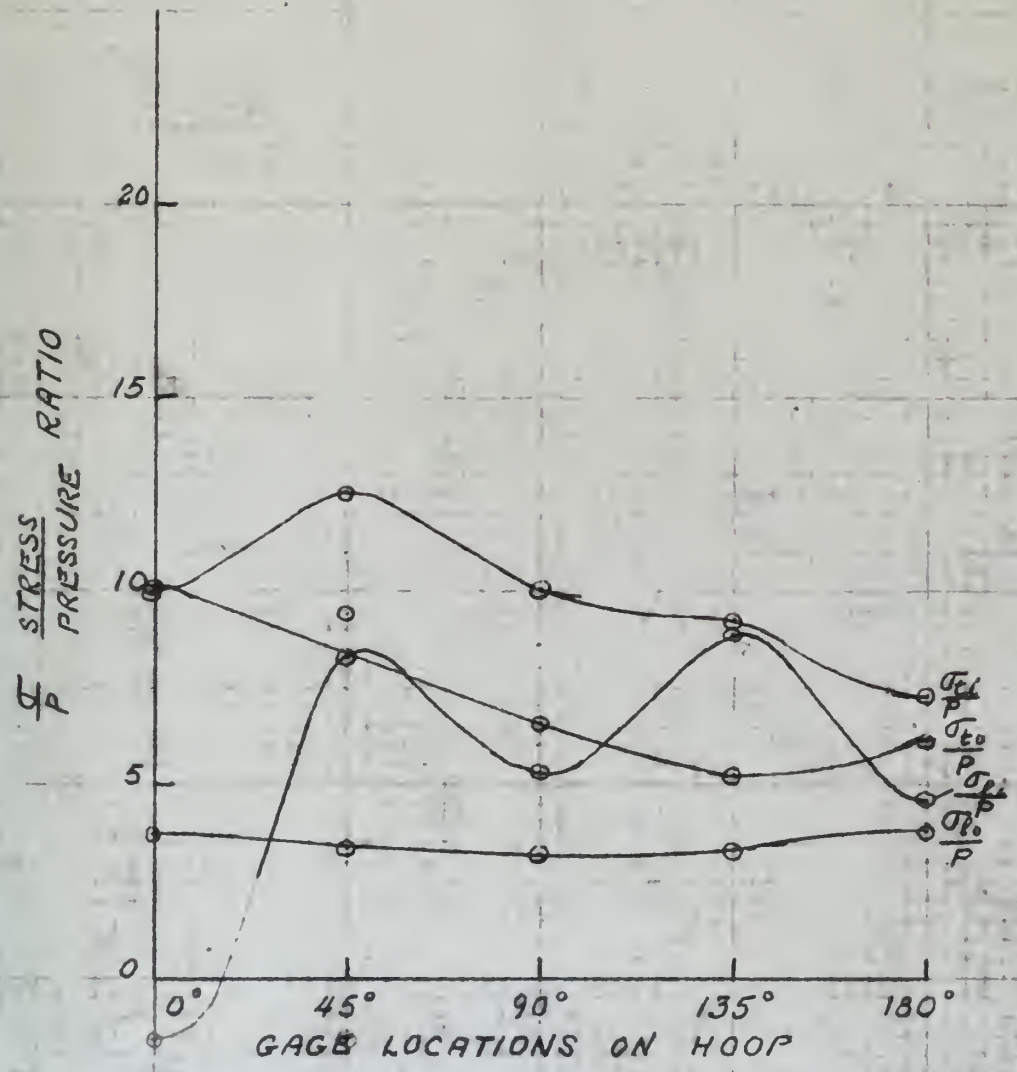

FIG. 14 SPECIMEN NO.4 SYMMETRICAL CROSS SECTION
STRESS TO PRESSURE VS. GAGE LOCATION

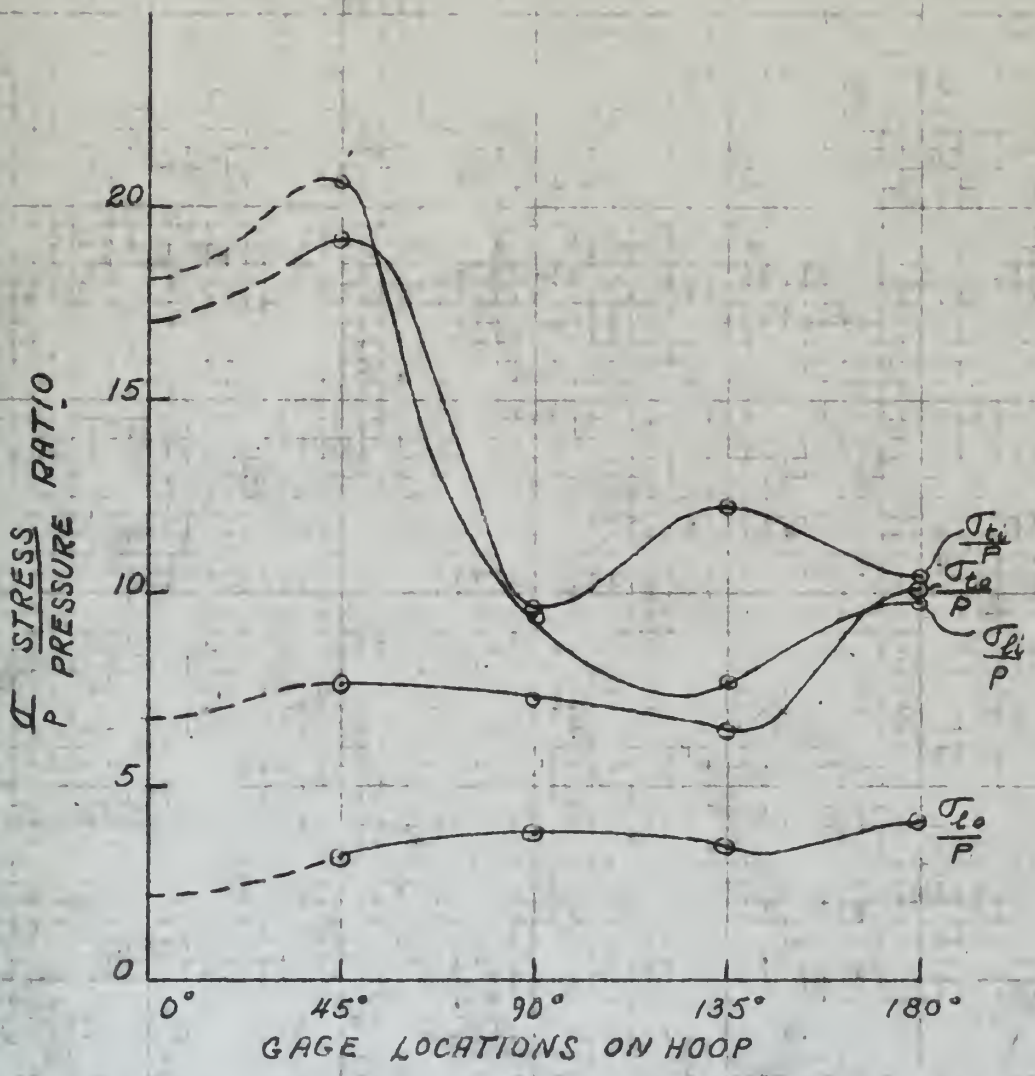

FIG. 15. SPECIMEN NO. 4 TRANSITION CROSS SECTION STRESS TO PRESSURE VS. GAGE LOCATION

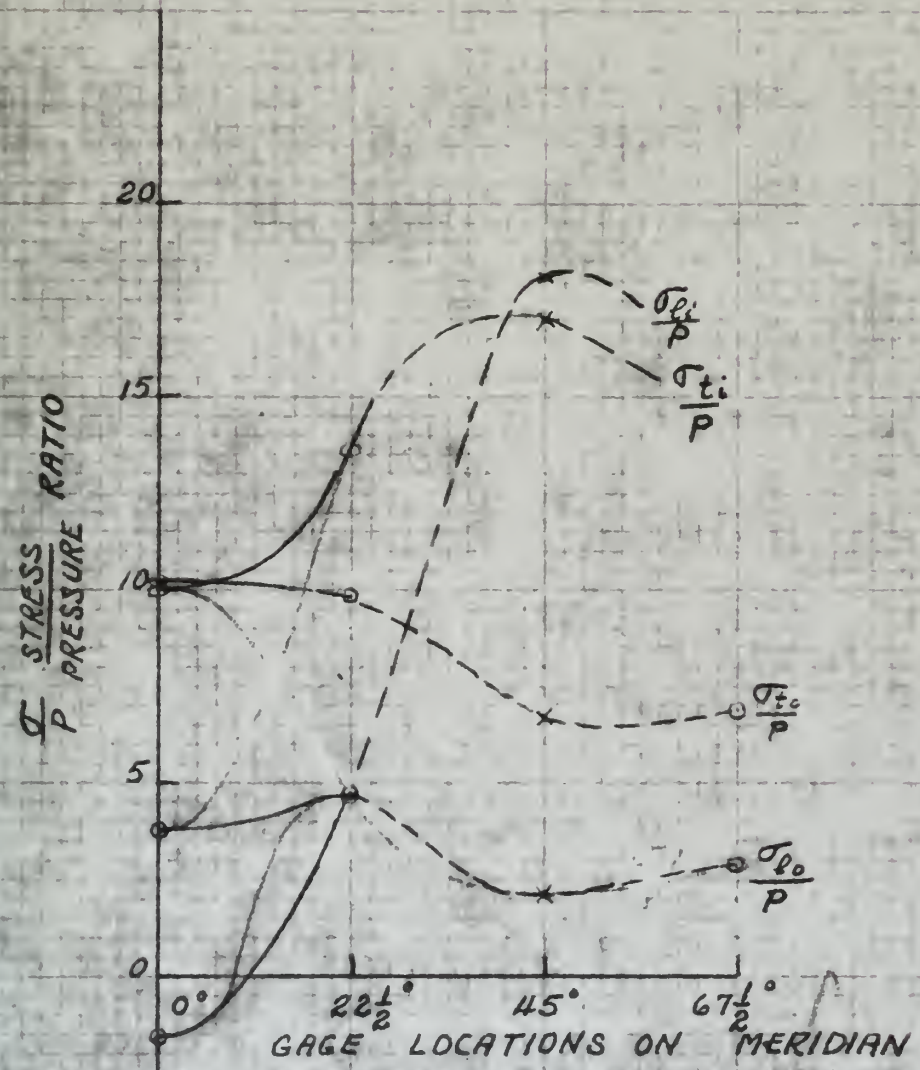

FIG. 16 SPECIMEN NO. 4 0° MERIDIAN
STRESS TO PRESSURE VS. GAGE LOCATION

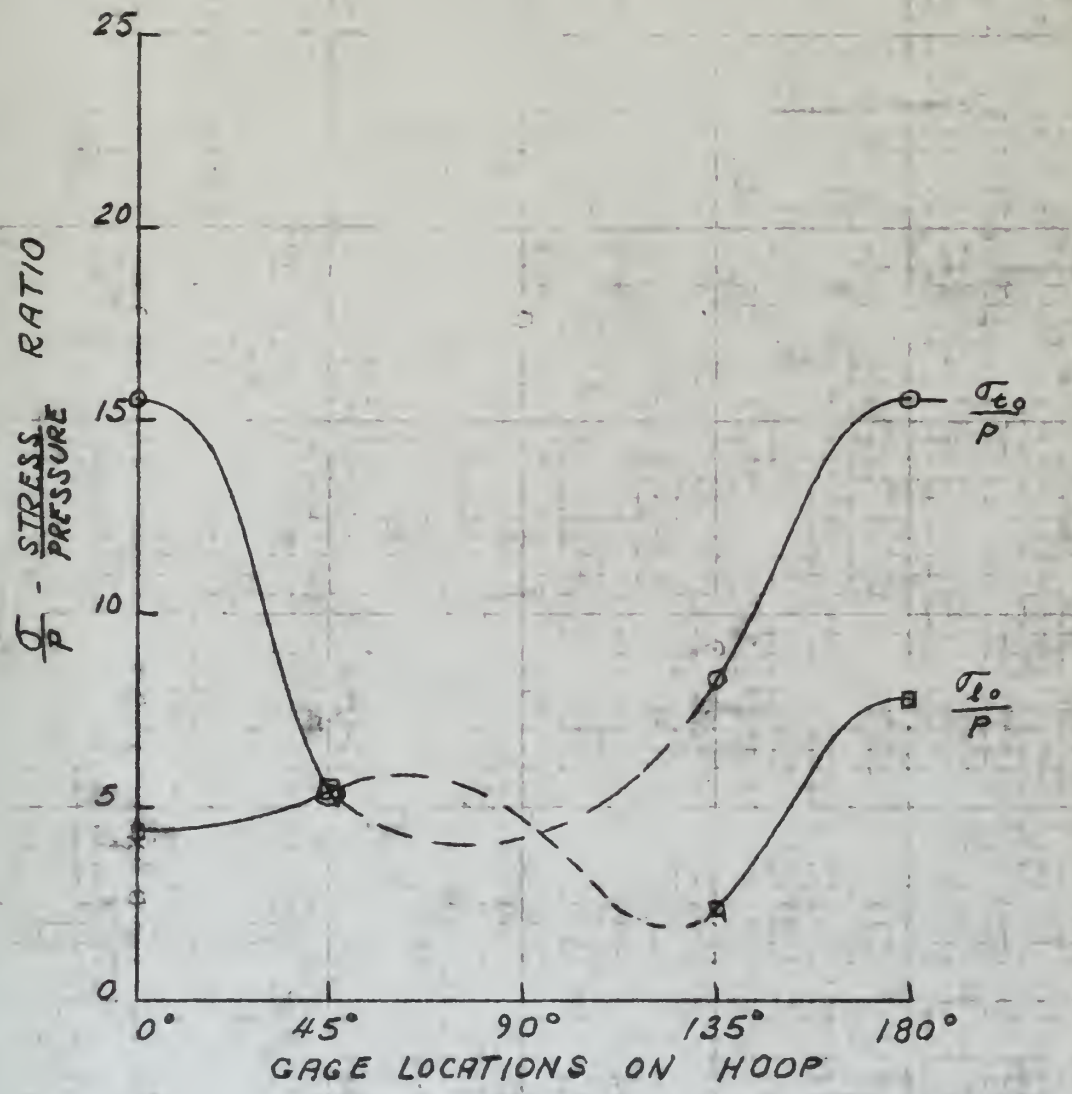

FIG. 17. SPECIMEN NO. 5 SYMMETRICAL CROSS SECTION
. STRESS TO PRESSURE VS. GAGE LOCATION

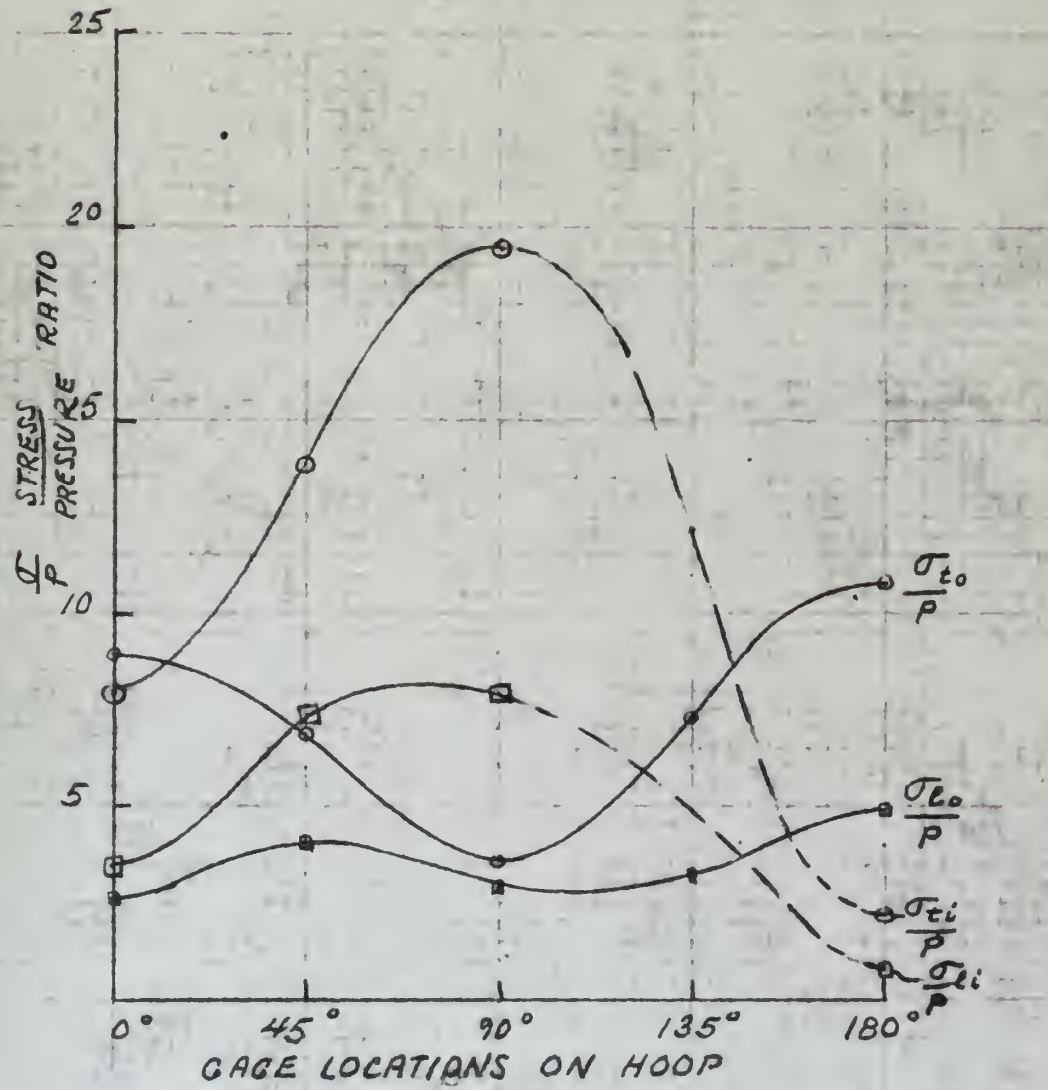

FIG. 18. SPECIMEN NO. 5 TRANSITION CROSS SECTION
STRESS TO PRESSURE VS. GAGE LOCATION

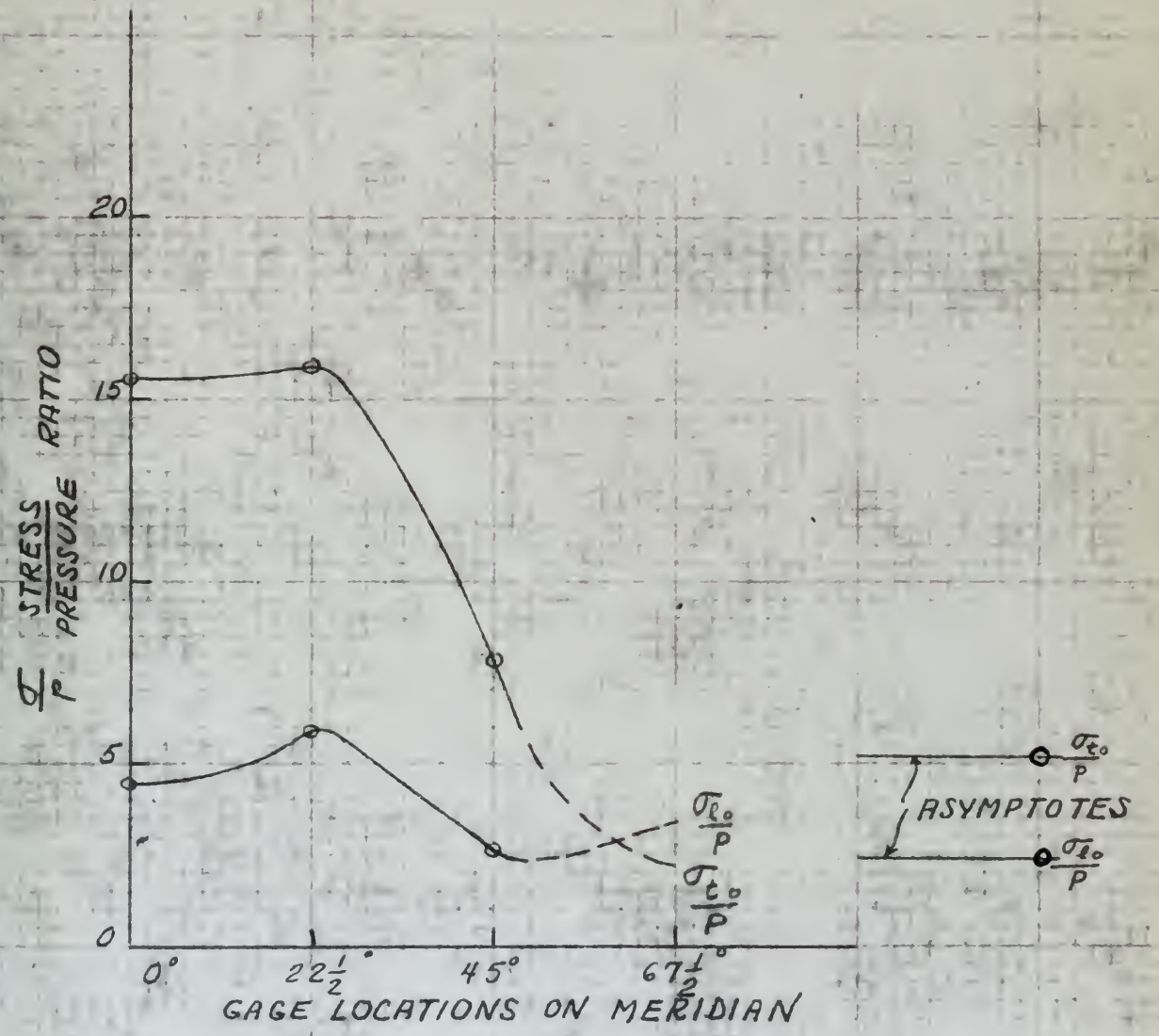

FIG. 17. SPECIMEN NO. 5 ON 0° MERIDIAN
STRESS TO PRESSURE VS. GAGE LOCATION

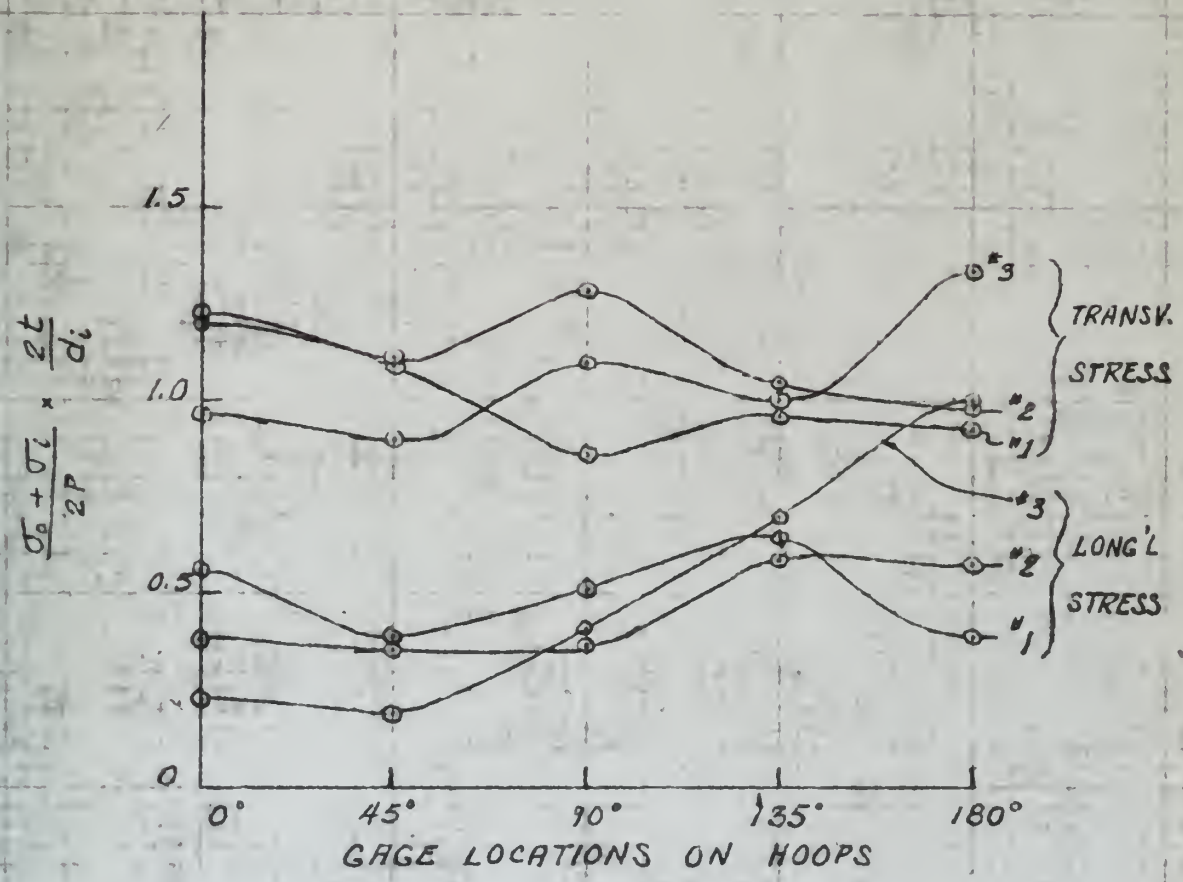

FIG. 20. SYMMETRIC CROSS SECTIONS
MEAN STRESS COEFFICIENT

R = thrust
t times

FIG.

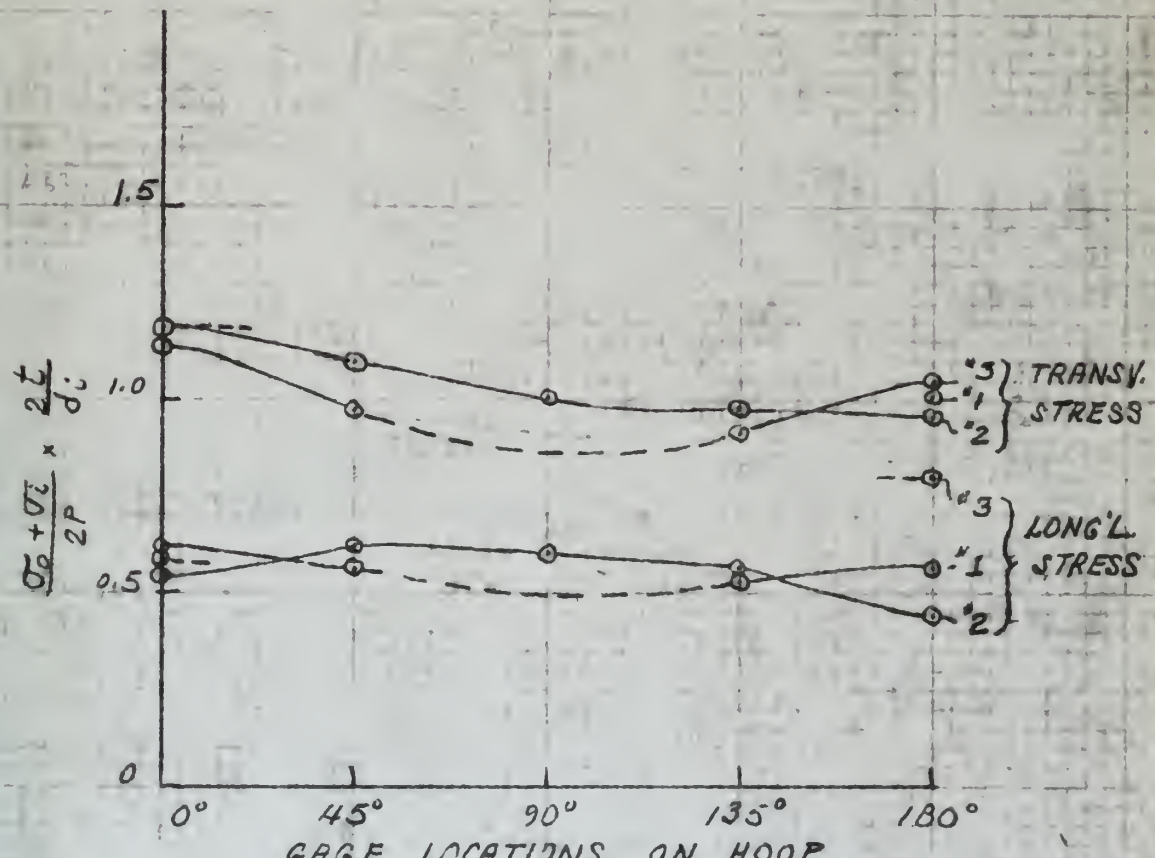

FIG. 21. TRANSITION CROSS SECTIONS
MEAN STRESS COEFFICIENT

FIG.

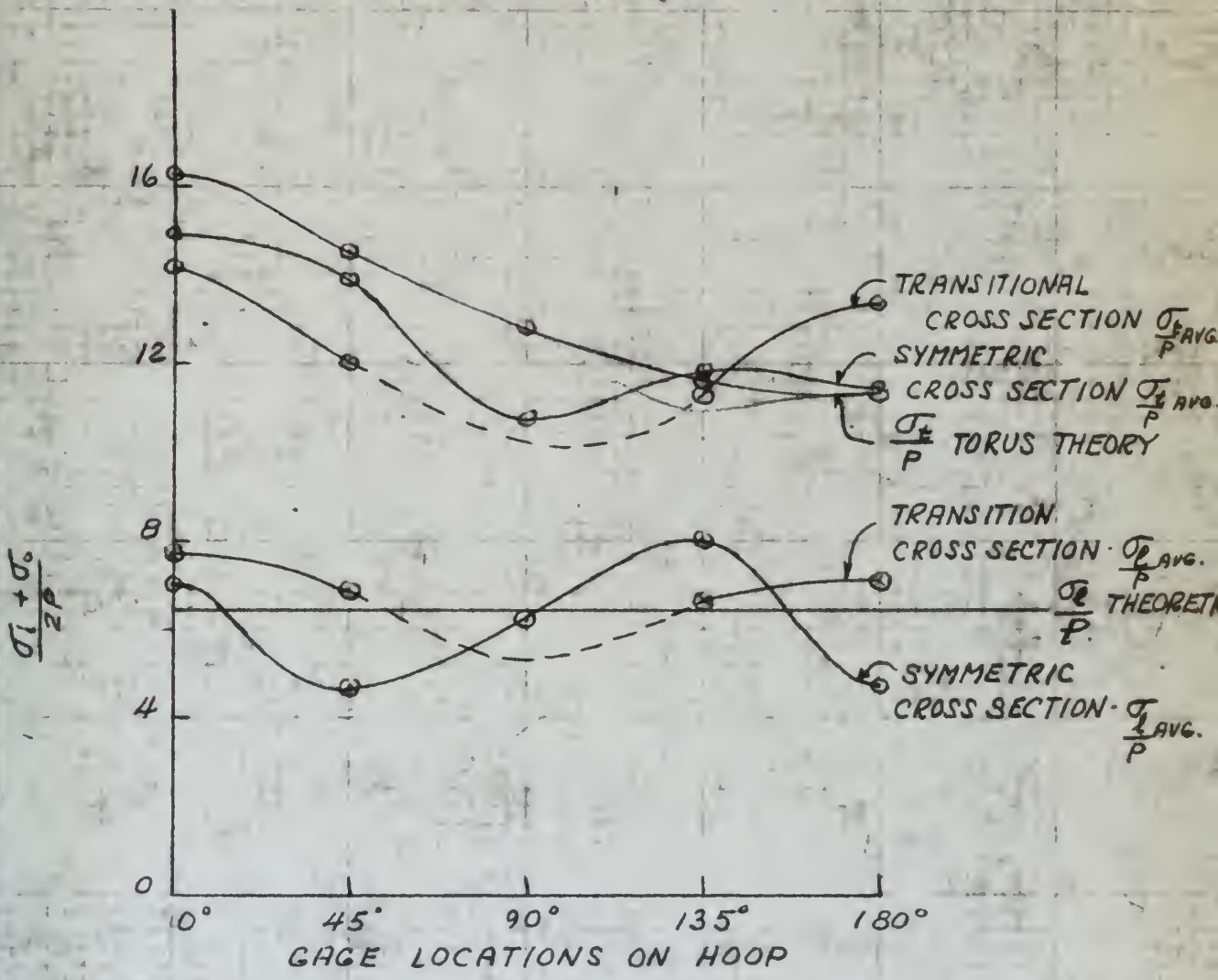

FIG. 22. SPECIMEN NO. 1

MEMBRANE STRESS TO PRESSURE VS. GAGE LOCATION

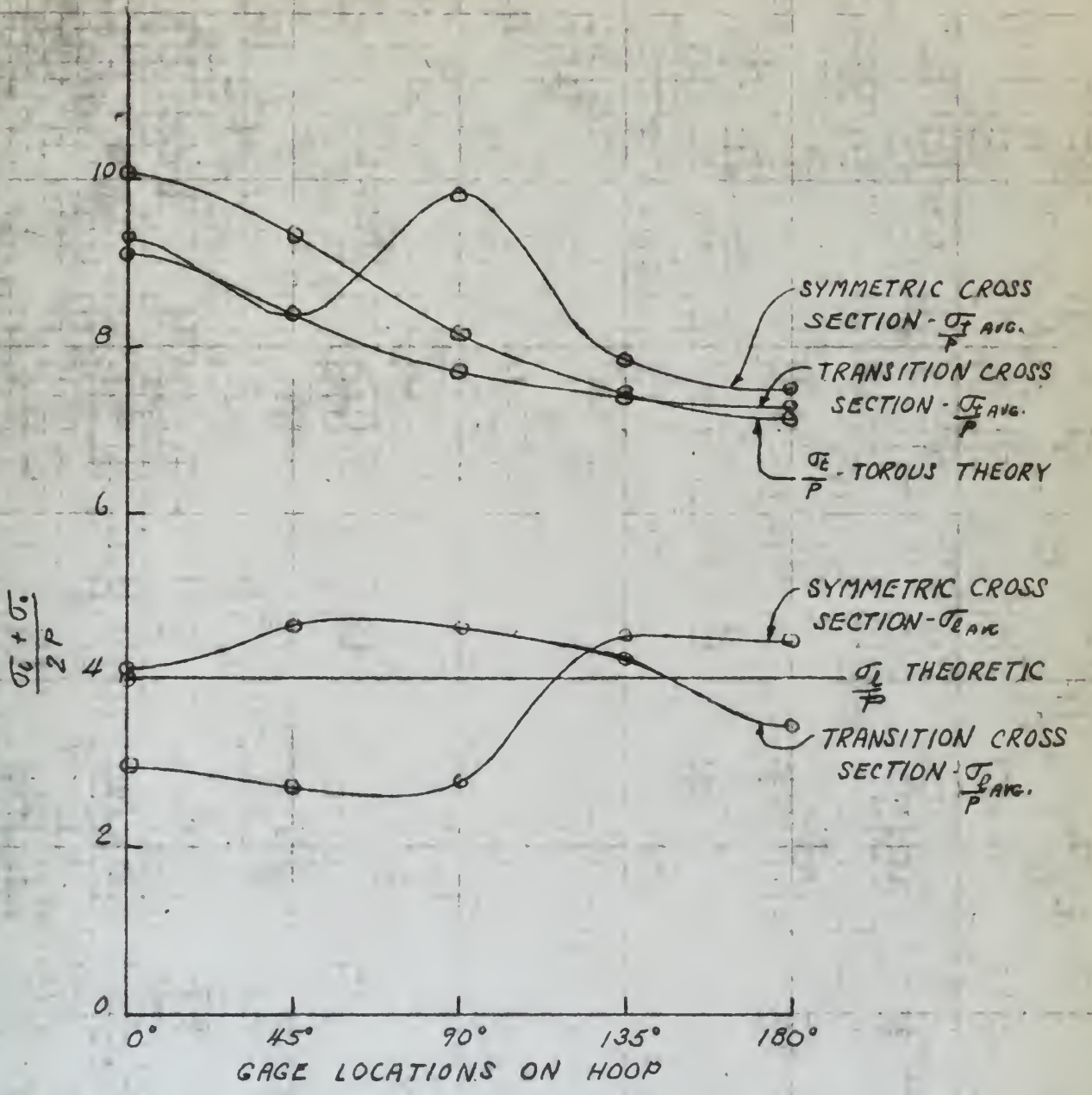

FIG. 23. SPECIMEN NO. 2 - MEMBRANE STRESS TO PRESSURE VS. GAGE LOCATION

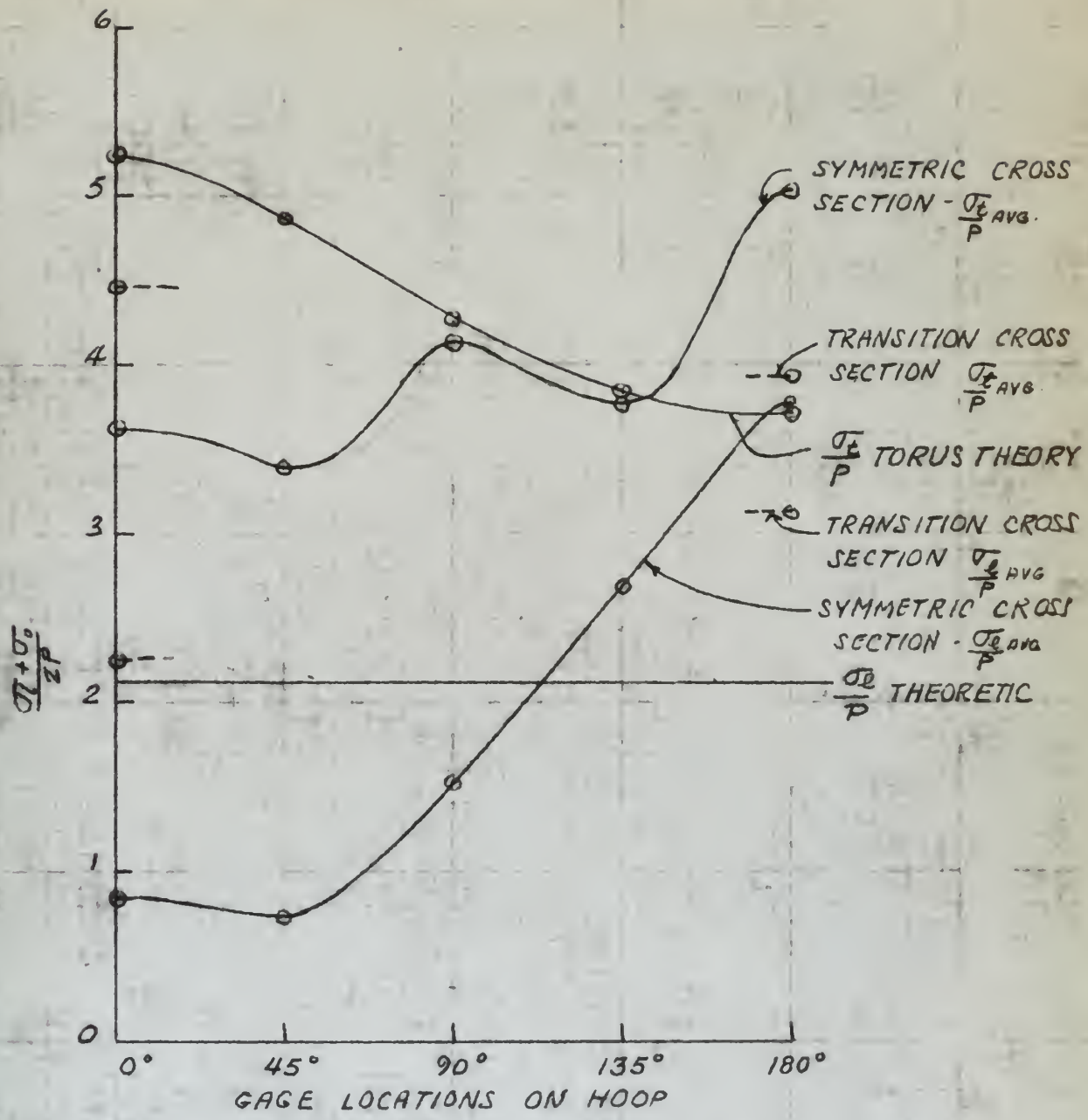

FIG. 24. SPECIMEN NO. 3. MEMBRANE STRESS TO PRESSURE VS. GAGE LOCATION

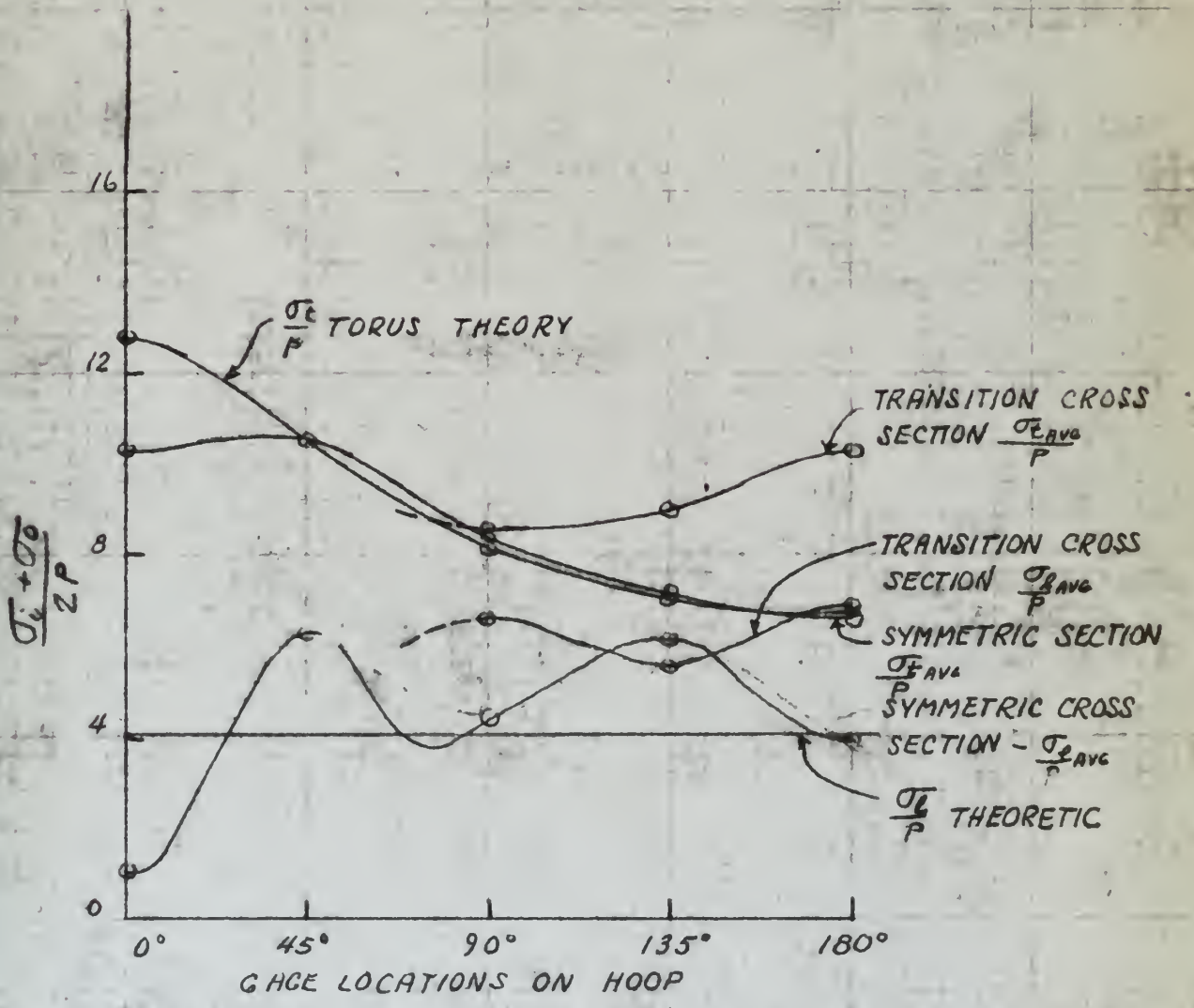

FIG. 25. SPECIMEN NO. 4. MEMBRANE STRESS TO PRESSURE VS. GAGE LOCATION

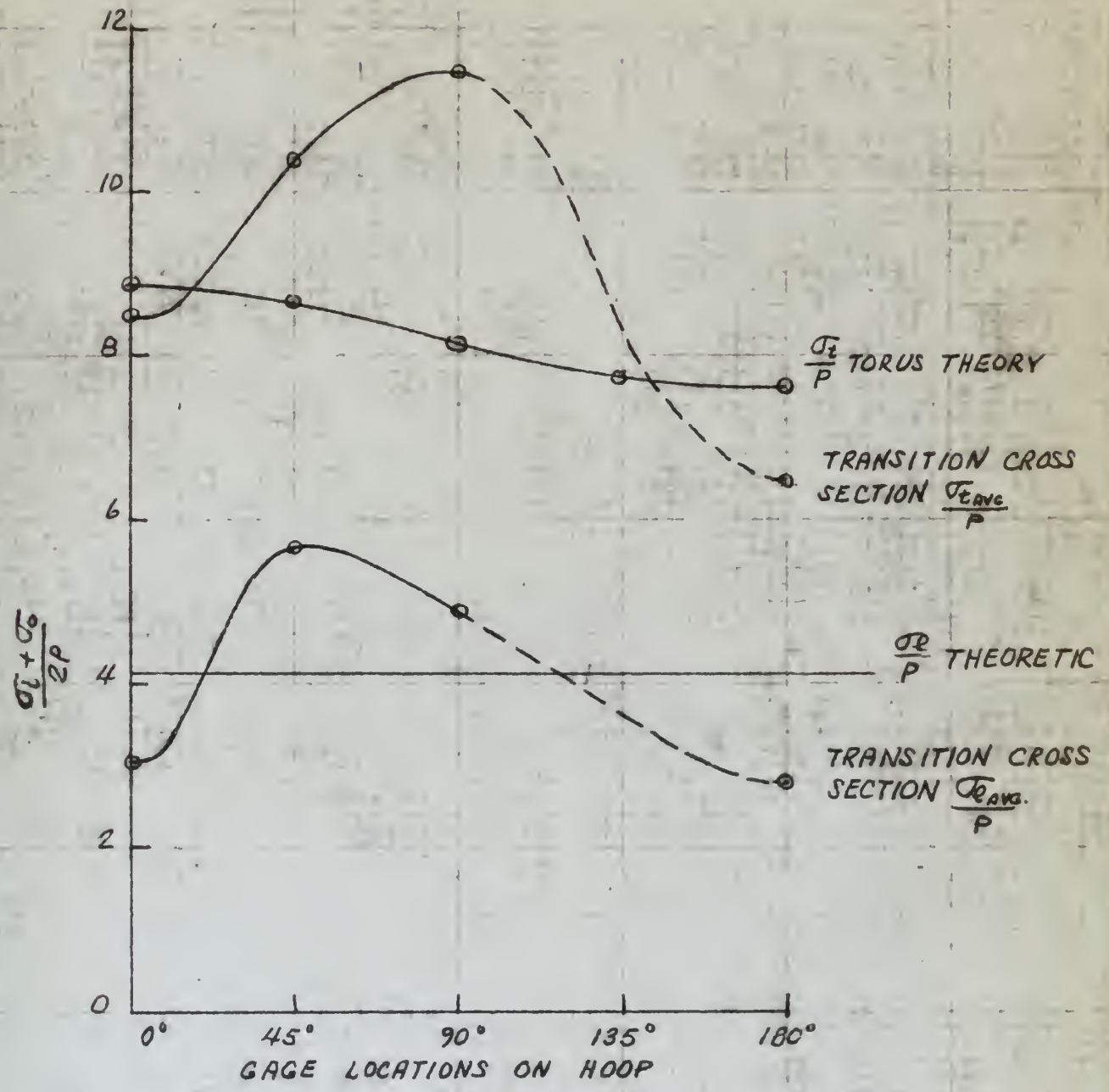

FIG. 26. SPECIMEN NO. 5. MEMBRANE STRESS TO PRESSURE VS. GAGE LOCATION

BIBLIOGRAPHY

1. Föeppl, A. Vorlesungen über technische mechanik III festighietslehre 228-229; München Verlag Von R. Oldenbourg, 1951.

2. Kooistra, L. F. and R. U. Blaser. Experimental Technique in Pressure-Vessel Testing. American Society of Mechanical Engineers. Transactions 72: 579-587. July 1950.

3. Lee, G. H. An introduction to experimental stress analysis. New York, John Wiley & Sons, Inc. 1950.

4. Meyer, H. C. E. Thicknesses of steam piping for high pressure, high temperature service. The Society for Naval Architects and Marine Engineers. Transactions 57: 379-399, July 1949.

5. O'Brien and E. Watterstrom. Discussion of Kooistra and Blaser 1 . American Society of Mechanical Engineers. Transactions 72: 587-588, July 1950.

6. Schoessow, G. J. and E. A. Brooks. Analysis of experimental data regarding certain design features of pressure vessels. American Society of Mechanical Engineers, Transactions 72: 567-577, July 1950

7. Timoshenho, S. Strength of Materials. Part 1, New York. McGraw Hill Book Co., 1951.

8. Timoshenho, S. and J. N. Goodier; Theory of Elasticity, New York. McGraw Hill Book Co., 1951.

9. U. S. Navy Bureau of Ships. Bureau of Ships Manual, Chapter 48. Washington, U. S. Government Printing Office, 1948.

1. [illegible]

2. [illegible]

3. [illegible]

4. [illegible]

5. [illegible]

6. [illegible]

7. [illegible]

8. [illegible]

9. [illegible]

APPENDIX I

FORMULAE (USING NOTATION - SEE PAGE ii)

1. LAMÉ SOLUTION - THICK WALLED STRAIGHT PIPE UNDER INTERNAL HYDROSTATIC PRESSURE

$$\frac{\sigma_t}{P} = \frac{r_i^2}{r_o^2 - r_i^2}\left(1 + \frac{r_o^2}{r^2}\right)$$

$$\frac{\sigma_{t\,max}}{P} = \frac{r_i^2 + r_o^2}{r_o^2 - r_i^2}, \quad \text{when } r = r_i$$

$$\frac{\sigma_l}{P} = \frac{r_i^2}{r_o^2 - r_i^2} \approx \frac{r_m}{2t} \quad \text{for membrane structure}$$

2. A. FÖPPL SOLUTION (MEMBRANE ANALYSIS OF TORUS).

$$\frac{\sigma_t}{P} = \frac{2R + r_m \sin\alpha}{R + r_m \sin\alpha} \times \frac{r_m}{2t} \quad \text{AT "A"}$$

$$\frac{\sigma_t}{P}_{max.} = \frac{2R + r_m}{R + r_m} \times \frac{r_m}{2t} \quad \text{AT "B"}$$

$$\frac{\sigma_l}{P} = \frac{r_m}{2t} \quad \text{AT ANY POINT}$$

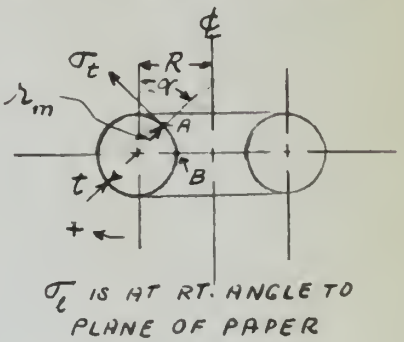

3. MEMBRANE ANALYSIS (STRAIGHT PIPE).

$$\frac{\sigma_t}{P} = \frac{r_m}{t}$$

$$\frac{\sigma_l}{P} = \frac{r_m}{2t}$$

APPENDIX II. SAMPLE PRESSURE VS STRAIN PLOT FOR TYPE AR-1 GAGE

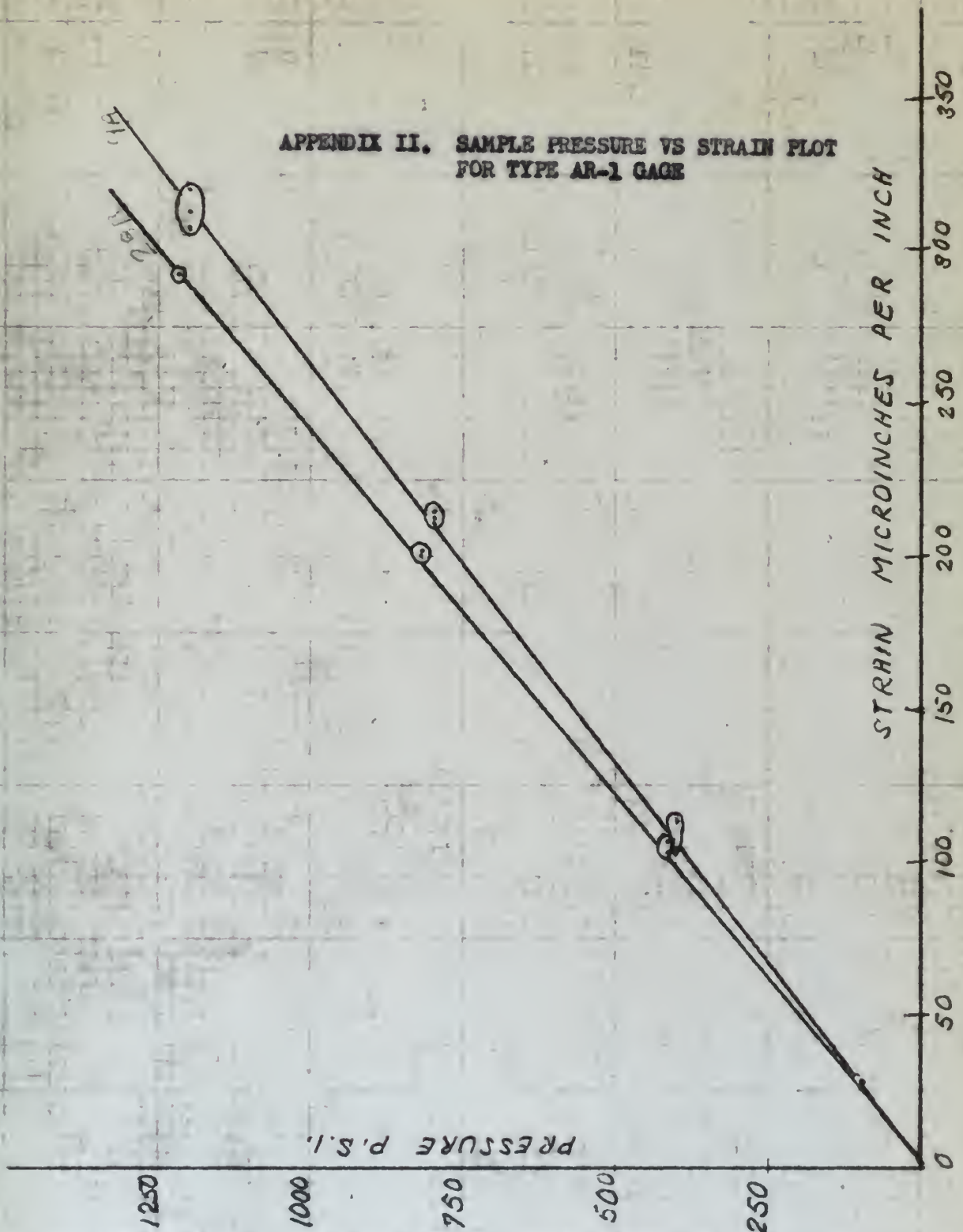

APPENDIX II SPECIMEN 1 MEASURED STRAIN - MICROINCHES PER INCH. INTERNAL PRESSURE VS STRAIN GAGES 28 B AND 7 B SAMPLE DATA GRAPH

APPENDIX III SAMPLE PRESSURE VS STRAIN PLOT FOR TYPE AX-5 GAGES

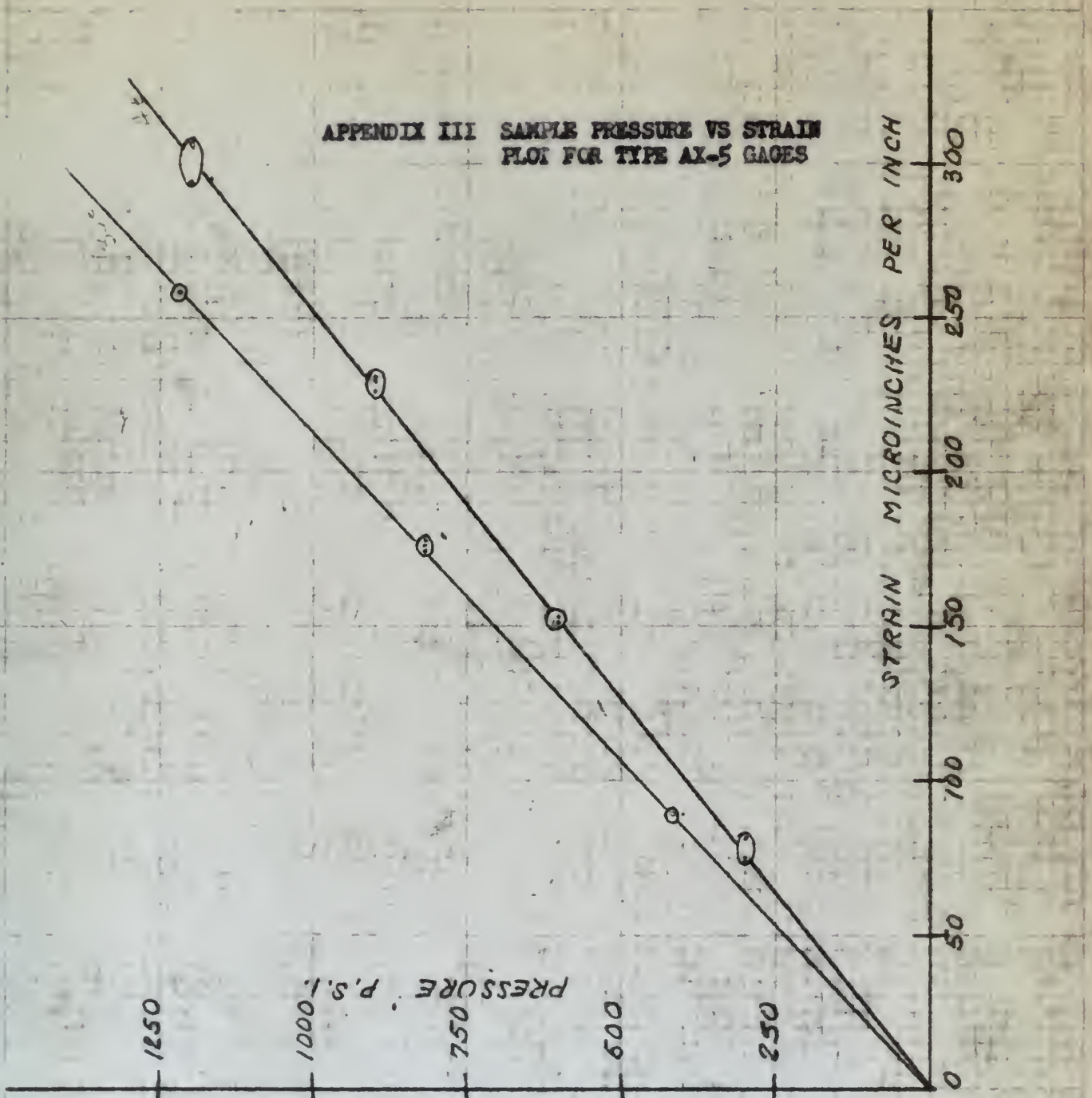

APPENDIX III SPECIMEN 4 MEASURED STRAIN MICROINCHES PER INCH INTERNAL PRESSURE VS. STRAIN GAGES 3 t (CONTROL) & GAGE 4 t SAMPLE DATA GRAPH

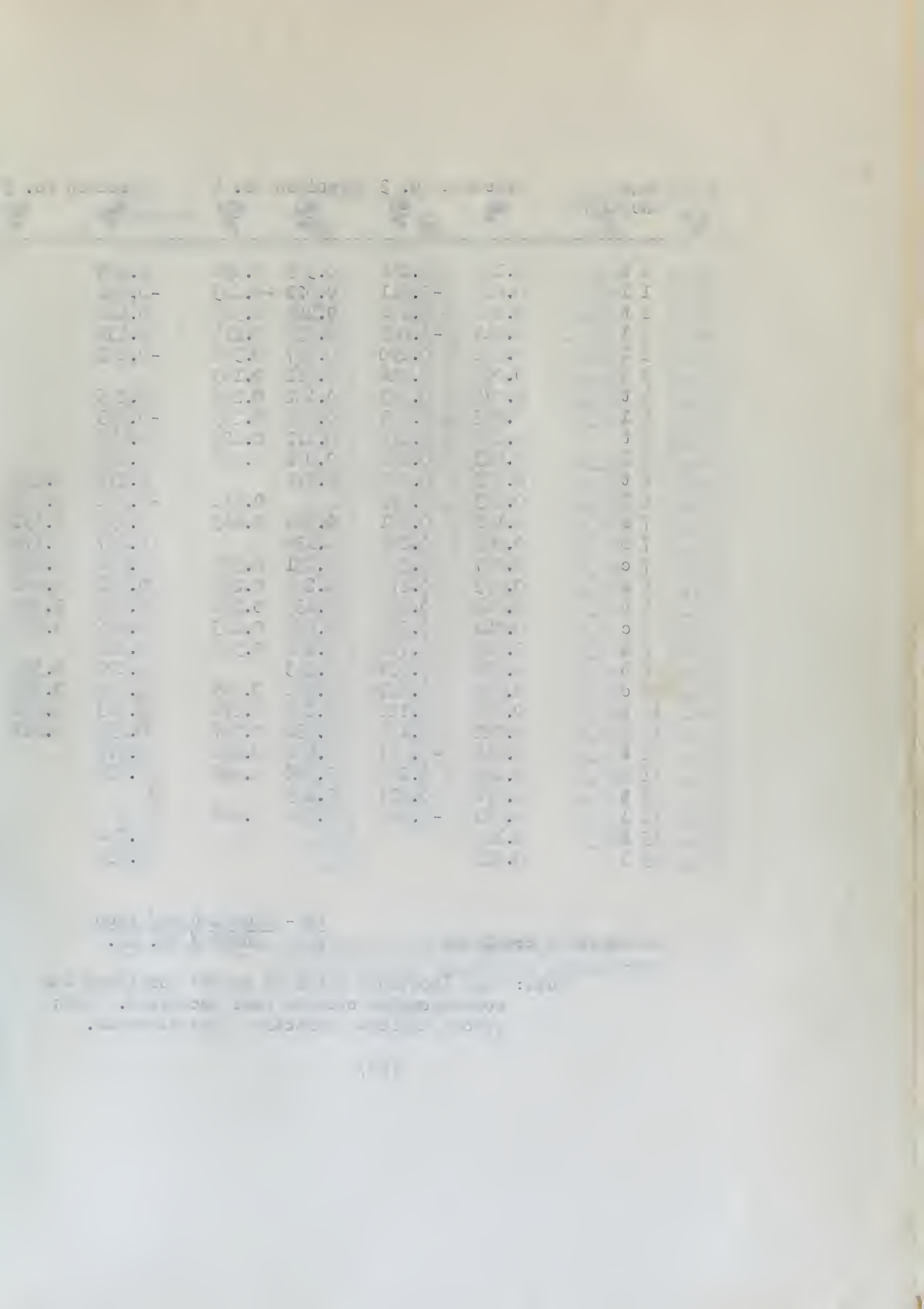

Gage Location	Specimen No. 3 $\frac{\epsilon_o}{p}$	Specimen No. 3 $\frac{\epsilon_i}{p}$	Specimen No. 4 $\frac{\epsilon_o}{p}$	Specimen No. 4 $\frac{\epsilon_i}{p}$	Specimen No. 5 $\frac{\epsilon_o}{p}$	Specimen No. 5 $\frac{\epsilon_i}{p}$
1 t	0.104	0.148	0.305	0.356	0.480	
1 l	0.018	-0.011	0.022	-0.123	-0.008	
2 t	0.100	0.136	0.245	0.355	0.126	
2 l	0.011	-0.005	0.030	0.214	0.131	
3 t	0.082	0.190	0.187	0.308	-0.102	
3 l	0.026	0.016	0.052	0.103		
4 t	0.074	0.153	0.142	0.245	0.255	
4 l	0.023	0.101	0.059	0.233	-0.003	
5 t	0.068	0.219	0.172	0.221	0.445	
5 l	0.023	0.155	0.052	0.106	0.108	
6 t	0.102	0.185	0.272		0.275	0.252
6 l	0.023	0.029		0.111	-0.001	0.060
7 a	0.102	0.581	0.224	0.463	0.195	0.131
7 b	0.065	0.299	0.136		0.157	0.179
7 c	0.017	0.365	0.031	0.525	0.066	0.420
8 a	0.093	0.270	0.205	0.255	0.092	0.096
8 b	0.064	0.484	0.135	0.241	0.085	0.354
8 c	0.021	0.353	0.055	0.243	0.065	0.594
9 a	0.089	0.775*	0.182	0.360	0.213	
9 b	0.056	0.537*	0.113		0.122	0.325
9 c	0.025	0.557*	0.051	0.159	0.036	0.350
10 t	0.070	0.122	0.298	0.276	0.313	0.088
10 l	0.012	0.154	0.034	0.247	0.056	0.027
11 t	0.016	-0.077	0.286	0.441	0.479	
11 l	0.105	0.248	0.056	0.028	0.035	
12 t	0.090	0.227	0.203			
12 l	0.021	-0.005	0.029	0.122		
13 t	0.100				0.146	
13 l	0.025				0.032	

APPENDIX IV continued

$\frac{Eo}{p}$ - $\frac{\text{microinches/ inch}}{\text{pounds/ sq. in.}}$

Note: Gage locations refer to inside locations and corresponding outside gage locations. Blank spaces indicate defective gage elements.

Gage Location	Specimen No. 1		Specimen No. 2	
	$\frac{\epsilon_a}{p}$	$\frac{\epsilon_t}{p}$	$\frac{\epsilon_a}{p}$	$\frac{\epsilon_t}{p}$
1 t	0.322	0.536	0.336	0.259
1 l	0.074	0.132	-0.008	0.036
2 t	0.336	0.531	0.260	0.277
2 l	-0.005	0.070	-0.010	0.046
3 t	0.368	0.252	0.434	0.201
3 l	0.087	0.146	-0.003	0.013
4 t	0.276	0.391	0.284	0.177
4 l	0.135	0.192	0.118	0.053
5 t	0.244	0.464		0.198
5 l	0.040	0.067	0.144	0.066
6 t	0.297	0.529	0.307	0.248
6 l	0.054	0.204	0.071	0.047
7 a	0.048	0.312	0.323	0.231
7 b	0.197	0.208	0.407	0.136
7 c	0.326	0.254	0.446	0.049
8 a	0.051	0.354	0.267	0.184
8 b	0.228	0.616	0.186	0.146
8 c	0.384	0.393	0.110	0.009
9 a	0.102	0.251	0.476	0.197
9 b	0.203	0.140	0.505	0.141
9 c	0.297	0.254	0.457	0.070
10 t	0.264	0.518	0.254	0.195
10 l	0.058	0.180	0.064	0.043
11 t	0.247	0.741	0.417	0.255
11 l	0.047	0.190	0.036	0.036
12 t	0.249	0.553	0.356	0.201
12 l	0.082	0.209	0.140	0.048
13 t	0.364		0.364	0.200
13 l	0.077			0.053

APPENDIX IV. OBSERVED STRAIN TO PRESSURE RATIO
(Corrected for transverse sensitivity)

Gage Location	Specimen No. 1		Specimen No. 2		Specimen No. 3	
	$\frac{\sigma_o}{p}$	$\frac{\sigma_i}{p}$	$\frac{\sigma_o}{p}$	$\frac{\sigma_i}{p}$	$\frac{\sigma_o}{p}$	$\frac{\sigma_i}{p}$
1 t	11.20	17.70	8.74	9.83	3.56	3.71
1 l	5.55	8.52	3.69	2.02	1.60	0.09
2 t	10.90	16.95	9.43	7.35	3.37	3.38
2 l	3.11	6.46	4.21	1.21	1.33	0.17
3 t	12.80	8.61	6.64	13.03	2.92	5.35
3 l	6.42	6.20	2.38	3.14	1.65	1.37
4 t	10.30	13.58	6.26	9.35	2.63	4.96
4 l	7.07	9.06	3.45	5.65	1.47	3.82
5 t	8.32	14.70	7.06		2.43	7.64
5 l	3.69	5.78	4.07		1.41	6.17
6 t	10.18	18.20	8.54	9.68	3.54	5.40
6 l	4.65	10.80	3.94	4.31	1.74	2.73
7 t	11.06	13.04	7.98	13.85*	3.49	21.48*
7 l	4.74	9.12	3.84	16.65*	1.55	16.55*
8 t	12.98	9.27*	6.66	8.75	3.22	11.21*
8 l	5.41	20.28*	4.06	5.19	1.59	13.10*
9 t	10.63	12.22	7.10	18.90*	3.14	29.62*
9 l	6.21	7.11	4.21	18.48*	1.68	24.62*
10 t	9.14	17.65	6.75	7.87	2.39	4.47
10 l	4.46	9.90	3.30	3.56	1.07	5.20
11 t	8.50	24.90	8.12	12.90	1.54	-1.84**
11 l	3.94	12.41	3.65	4.25	3.58	6.32
12 t	8.88	19.00	7.00	12.28	3.13	6.35
12 l	5.10	11.20	3.53	7.03	1.56	1.05
13 t	12.60		7.01		3.50	
13 l	6.05		3.67		1.79	

APPENDIX V. CALCULATED ACTUAL STRESS-TO-PRESSURE RATIO

Gage Location	Specimen No. 4		Specimen No. 5	
	σ_o/p	σ_i/p	σ_o/p	σ_i/p
1 t	10.10	10.02	15.53	
1 l	3.70	-1.52	4.42	
2 t	8.26	12.62	5.30	
2 l	3.37	9.40	5.48	
3 t	6.60	10.03		
3 l	3.52	5.36		
4 t	5.20	9.25	8.26	
4 l	3.31	8.96	2.35	
5 t	6.10	7.24	15.52	
5 l	3.38	4.61	7.85	
6 t			8.94	7.79
6 l			2.65	3.44
7 t	7.58	19.20*	6.98	13.90
7 l	3.19	20.60*	4.05	7.35
8 t	7.21	9.65	3.67	19.41*
8 l	3.79	9.40	2.98	7.91
9 t	6.42	12.25	7.27	
9 l	3.44	7.68	3.25	
10 t	10.02	10.38	10.70	2.12
10 l	4.02	9.70	4.88	0.73
11 t	9.91	13.60	15.90	
11 l	4.62	4.54	5.81	
12 t	6.87			
12 l	2.92			
13 t			5.06	
13 l			2.96	

APPENDIX V - continued

*the calculated stresses at these points are considered unreliable from equilibrium considerations of the stresses in the longitudinal direction.

**considered unreliable due to nature of reading.

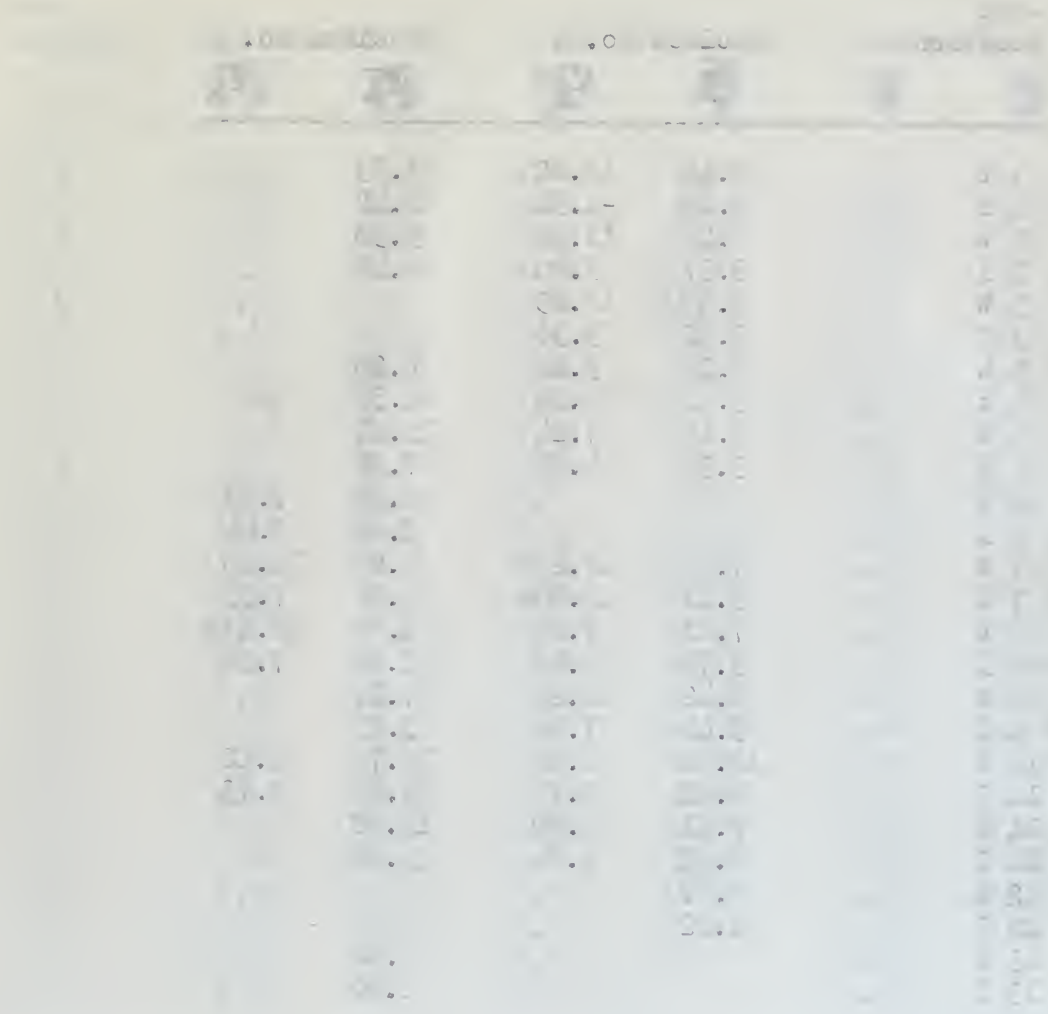

Location	Specimen No. 1		Specimen No. 2		Specimen No. 3		Specimen No. 4		Specimen No. 5	
	σ_1/p	σ_2/p	σ_1/p	σ_2/p	σ_1/p	σ_2/p	σ_1/p	σ_2/p	σ_1/p	σ_2/p
7_1	11.06	13.05	13.06	*	3.49	*	7.58	*	7.14	14.70*
7_2	4.74	9.11	9.09	*	1.55	*	3.19	*	3.90	6.54*
$t_{\theta 1}$	0°	3.75°	1.35°	*	-3.7°	*	0°	*	-18°	-25° *
8_1	12.98	20.30**	6.69	8.75	3.62	*	7.21	*	3.62	19.71
8_2	5.41	9.25**	4.03	5.19	1.58	*	3.79	*	2.98	7.61
$t_{\theta 1}$	0°	86.3°**	9.3°	0	-5.3°	*	-2°	*	0	-13.2°
9_1	10.63	12.22	7.11	*	3.14	*	6.42	*	7.27	*
9_2	6.21	7.11	4.20	*	1.68	*	3.44	*	3.25	*
$t_{\theta 1}$	0°	0°	3.1°	*	0.9°	*	0°	*	1°	*

(57)

* Insufficient data
** Unreliable data

APPENDIX VI Principal Stress-to-Pressure Ratios and Principal Stress Directions.

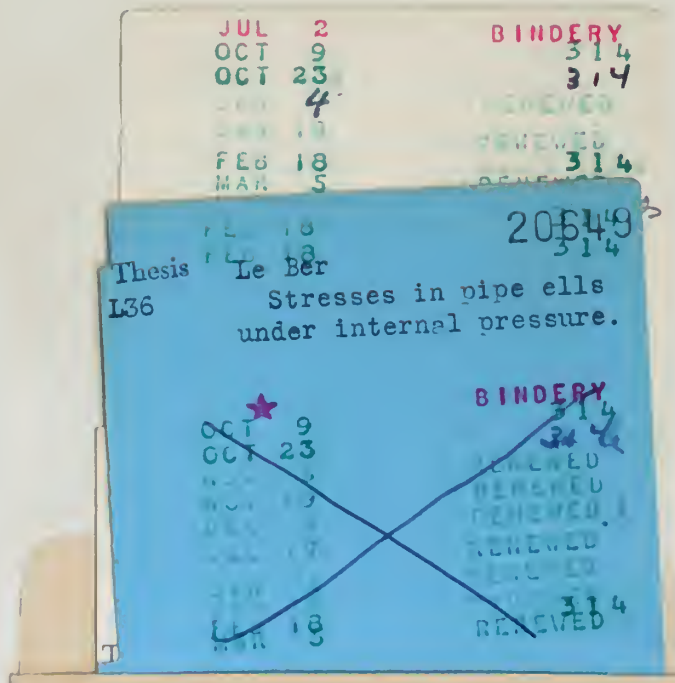

Thesis
L36
Le Ber
Stresses in pipe ells under internal pressure. .
20649

Library
U.S. Naval Postgraduate School
Monterey, California

ARTISAN
GOLD LETTERING
AND
SMITH BINDERY
OAKLAND, CALIF.

thesL36
Stresses in pipe ells under internal pre
3 2768 002 11979 4
DUDLEY KNOX LIBRARY C.1